Noname manuscript No.
(will be inserted by the editor)

Shock Structure in Extended Thermodynamics with Second Order Maximum Entropy Principle Closure ⋆

Andrea Mentrelli · Tommaso Ruggeri

Received: date / Accepted: date

Abstract An investigation on the features of the shock structure solution of the 13 moment system of Extended Thermodynamics with a second order closure based on the maximum entropy principle (MEP) is presented. The results are compared to those obtained by means of the traditional first order closure, and to those obtained in the framework of kinetic theory by solving the Boltzmann equation with a BGK model for the collision term.

It is seen that when adopting a second order closure, the strength of the subshock that appears in the shock structure profile for large enough Mach numbers is remarkably reduced with respect to what is found with the first order closure, and the overall profile of the shock structure solution is in better agreement with the results obtained with the kinetic theory approach. The analysis is extended to the case of the 14 moment system of a polyatomic gas and some preliminary results are presented also for this case.

Keywords Extended Thermodynamics · Shock structure · Maximum Entropy Principle

1 Introduction

The study of nonequilibrium phenomena in gases is particularly important. We have two complementary approaches, namely the *continuum approach* and the *kinetic one*. The continuum model consists in the description of the system using macroscopic equations (e.g., fluid-dynamic equations) obtained based on

⋆ Published on *Continuum Mechanics and Thermodynamics* (Springer); https://doi.org/10.1007/s00161-020-00892-2 (DOI: 10.1007/s00161-020-00892-2)

Andrea Mentrelli, Tommaso Ruggeri
Department of Mathematics & Alma Mater Research Center on Applied Mathematics, AM^2
University of Bologna
E-mail: andrea.mentrelli@unibo.it (corresponding author)
E-mail: tommaso.ruggeri@unibo.it

conservation laws and appropriate constitutive equations. A typical example is the Navier-Stokes and Fourier model in Thermodynamics of Irreversible Processes (TIP) that is based on the assumption of *local equilibrium*. Therefore the applicability of this theory is restricted to a nonequilibrium state characterized by a small Knudsen number K_n, which is a measure of the extent to which the gas is rarefied. The advantage of the continuum approach is that the range of validity is not restricted only to rarefied gases but includes also dense gases.

The approach based on the kinetic theory [1–3] postulates that the state of a gas can be described by the velocity distribution function, the evolution of which is governed by the Boltzmann equation. The kinetic theory applies to a nonequilibrium state characterized by a large K_n, therefore the range of the applicability of the Boltzmann equation is limited to rarefied gases.

Rational Extended Thermodynamics (RET) [4, 5] is a phenomenological theory that can be regarded as a generalization of TIP, thus belonging to the class of continuum models, but beyond the assumption of local equilibrium. The systems of first-order balance laws that characterize RET can indeed be interpreted as systems of moment equations obtained form the Boltzmann equation. Because of this intrinsic feature, RET offers the promise of applying to non-equilibrium states with larger Knudsen numbers, with respect to the range of applicability of classical continuum models; RET can, therefore, be regarded in the case of rarefied gas as a bridge between TIP and kinetic theory, allowing to take advantage of tools and considerations of kinetic theory when, for instance, the problem of the closure is faced.

The original approach of RET to the problem of the closure is based on universal principles of continuum physics, i.e. the entropy principle, the principle of objectivity and the principle of thermodynamical stability. This approach, which turns out to be equivalent in the 13-moment case to the closure approach used by Grad motivated by kinetic theory [6], can be replaced by the approach based on the Maximum Entropy Principle (MEP), which was proven to be equivalent to the original continuum approach [7, 8], but more amenable to be used when a large number of moments are considered.

The MEP, developed by Jaynes in the context of the theory of information [9, 10], was first adopted for the closure of the system of moment equations by Kogan [11], then Müller and Ruggeri in the first edition of their book proved that the closure of MEP gives a symmetric hyperbolic system [8]. The complete equivalence between the closures obtained by means of the entropy principle and by means of the MEP was later proved by Boillat and Ruggeri [12] who considered a general entropy functional valid for any kind of rarefied gases including degenerate gases as Fermions or Bosons (see also [4]).

Nevertheless the MEP usually is exploited in RET in a different way with respect to traditional MEP-based theories: the solution of the entropy maximization problem is sought only in the neighborhood of the local equilibrium, and in the standard formulation the resulting model equations are linear in non-equilibrium variables. When rational extended thermodynamics is combined with the maximum entropy principle, the resulting theory – denoted as

Molecular Extended Thermodynamics (MET) [8] – is free from the issues affecting traditional theories of closure of moment equations in non-linear case: i) non convergence of the moments for any truncation order [12, 13] and ii) the domain of definition of the flux of the last moment equation is not convex, the flux has a singularity, and the equilibrium state lies on the border of the domain of definition of the flux [14].

These benign features of the linear MEP-based closure come at a price, though. In addition to the fact that the validity of the theory is now limited by construction to the neighborhood of the local equilibrium state, the resulting system of equations loses the property of global hyperbolicity; a major consequences is a reduced hyperbolicity region.

Moreover as the systems of RET are hyperbolic with a convex entropy density (at least in some region in the neighborhood of equilibrium) then for a theorem due to Boillat and Ruggeri [15] there exists always a subshock when the shock speed exceeds the non perturbed equilibrium maximum characteristic velocity. These appear as "artificial" discontinuities, at least for a monatomic gas, since no evidence of such discontinuities are seen in experimental results. The situation is quite different in polyatomic gas [5].

The loss of global hyperbolicity of its first-order balance law system, has recently been reconsidered by Brini and Ruggeri [16], with an investigation of the effects on the hyperbolicity property of a second order closure, rather than the standard first order one, in the context of the 13 moment system of a monatomic gas. The result of the analysis presented in [16] is that a second order formal expansion of the distribution function about the local equilibrium results in an extension of the hyperbolicity region. This result, apart from being interesting in its own right from a mathematical standpoint, is especially interesting because it shows that the long-standing issue of the reduced hyperbolicity region affecting RET theories can be addressed in the framework of the theory itself: An increase of the order of the formal expansion of the distribution function in the procedure of the closure of the system via-MEP, possibly accompanied by an increase in the number of moments of the truncated system, hopefully leads to a matching increase of the hyperbolicity region.

The result presented in [16] legitimately renews the interest in MET and leads quite naturally to another question: How does a second order closure affect the shock-structure solution far from equilibrium? In other words: Is a second-order closure beneficial also in relation to the other of the two major issues of MET theories mentioned earlier, i.e. the formation of artificial discontinuities in the solution?

The purpose of the present paper is to start an investigation in this direction. The features and the behaviors of the shock-structure solution are analyzed for the one-dimensional 13 moment system when first and second order MEP-based closures are exploited. In particular, the shock-structure solution obtained with these two closures for increasing strength of the shock are compared in order to investigate how the higher order closure impacts on the

characteristic of the well-known subshock that affects the solution far enough from equilibrium.

It will be shown that a second order closure is beneficial also from the point of view of the reduction of the subshock strength which appears in far-from-equilibrium processes. In the sequel of the paper it will be presented a comparison of the shock structure solution for the 13 moment system obtained with the standard first order closure, the novel second order closure, and obtained by means of kinetic theory, i.e. solving the Boltzmann equation with the collision term given by the BGK model, which is consistent with the model upon which the moment equations are based. The comparison will reveal that the second order MEP-based closure provides predictions that are in better agreement with those obtained with kinetic theory.

Finally, the analysis will be extended to the 14 moment theory of a polyatomic gas.

As a follow-up to this study, a first step towards the analysis of higher order MEP-based closures in the case of the 14 moment system of extended thermodynamics will be the subject of a forthcoming paper [17].

The rest of the paper is organized as follows. In Section 2, the maximum entropy principle and its application in extended thermodynamics are reviewed. The algorithm that allows to obtain the closing fluxes for any arbitrary order of the closure is described following [16, 18] and its specialization to the one-dimensional case is described in Section 2.1, along with a step-by-step application of the procedure to the case of the 13 moment system discussed in the rest of the paper.

In Section 3, the 13 moment system of a monatomic gas is recalled and the expressions of the closing fluxes that are obtained exploiting the maximum entropy principle with the first and second order closures are given for the one-dimensional case, following the results outlined in Section 2.1.

In Section 4, the basic theory of the shock structure solution of a first-order balance law system is recalled, and the system of ordinary differential equations that allow to obtain such a solution in the case of the 13 moment system of a monatomic gas are provided for both the first order closure (Section 4.1) and the second order closure (Section 4.2).

In Section 5, the Rankine-Hugoniot compatibility conditions that permit to analyze the subshock formation in the case in which the shock structure solution is not continuous are given for both the first order closure (Section 5.1) and the second order closure (Section 5.2).

In Section 6, a selection of the numerical results obtained for the shock structure solution of the 13 moment system of a monatomic gas for various Mach numbers are shown. The results are compared to those obtained solving the Boltzmann equation with the BGK approximation for the collision term.

In Section 7, the 14 moment system for a polyatomic gas is recalled and the closing fluxes obtained for this system when the first and second order closures are exploited are provided in Section 7.1 and 7.2, respectively. In Section 7.3, a non-exhaustive preliminary comparison of the shock structure

solution computed for the 14 moment system of polyatomic gases with first and second order closures, as well as with the Boltzmann/BGK model equation, is presented.

Finally, in Section 8, some concluding remarks on the present investigation are outlined.

2 Maximum Entropy Principle and Molecular Extended Thermodynamics of degree α

The mathematical structure of RET has a strict connection with kinetic theory, as its system of partial differential equations can be related to the system of equations obtained taking suitable moments of the Boltzmann equation.

For a rarefied monatomic gas, the Boltzmann equation is an evolutionary equation for the distribution function $f(\mathbf{x}, \mathbf{c}, t)$, where $f(\mathbf{x}, \mathbf{c}, t)\, d\mathbf{c}$ represents the number of molecules which at time t have position $\mathbf{x}$ and velocity between $\mathbf{c}$ and $\mathbf{c} + d\mathbf{c}$. In the general case of molecules with three degrees of freedom, such that $\mathbf{x} \equiv (x_1, x_2, x_3) \in \mathbb{R}^3$ and $\mathbf{c} \equiv (c_1, c_2, c_3) \in \mathbb{R}^3$, the Boltzmann equation reads

$$\partial_t f + c_i \partial_i f = Q, \tag{1}$$

where ∂_t denotes the partial derivative with respect to time t, ∂_i the partial derivative with respect to the spatial coordinate x_i $(i = 1, 2, 3)$, and Q is the term accounting for the effects on the distribution function f of the collisions between particles (collision term).

Introducing the velocity moments of the distribution function f:

$$F = \int mf \, d\mathbf{c}, \quad F_{k_1 k_2 \cdots k_j} = \int mf c_{k_1} c_{k_2} \cdots c_{k_j} \, d\mathbf{c}, \\ (k_1, k_2, \ldots k_j = 1, 2, 3, \quad j \geqslant 1),$$

and of the collision term Q (production terms):

$$P_{k_1 k_2 \cdots k_j} = \int mQ c_{k_1} c_{k_2} \cdots c_{k_j} \, d\mathbf{c} \qquad (j \geqslant 2),$$

where m denotes the mass of a molecule, and the integrals are intended over the three-dimensional velocity-space $\mathbb{R}^3$, an infinite hierarchy of first-order tensorial balance laws of increasing rank can be obtained, in which the flux in

one equation appears as density in the following one:

$$
\begin{aligned}
&\partial_t F + \partial_i F_i = 0, \\
&\partial_t F_{k_1} + \partial_i F_{ik_1} = 0, \\
&\partial_t F_{k_1k_2} + \partial_i F_{ik_1k_2} = P_{\langle k_1k_2\rangle}, \\
&\partial_t F_{k_1k_2k_3} + \partial_i F_{ik_1k_2k_3} = P_{k_1k_2k_3}, \\
&\quad\vdots \\
&\partial_t F_{k_1k_2\cdots k_N} + \partial_i F_{ik_1k_2\cdots k_N} = P_{k_1k_2\cdots k_N}, \\
&\quad\vdots
\end{aligned}
\tag{2}
$$

where $P_{\langle k_1k_2\rangle} = P_{k_1k_2} - \frac{1}{3}P_{ll}\delta_{k_1k_2}$ is the deviatoric part of the tensor $P_{k_1k_2}$ and it has been taken into account that the first, the second and the trace of the third tensorial equations of this hierarchy represent, respectively, the conservation laws of mass, momentum and energy and, as such, they have null production terms (the weights 1, c_k, $c^2 = c_lc_l$ appearing in the first five moments of the collision term are the so-called *collision invariants*).

Let us now consider the system obtained from (2) by taking the equations with densities up to the one with N indexes and let us introduce the vector of generating weights

$$
\boldsymbol{\Phi} = (1,\, c_{k_1},\, c_{k_1}c_{k_2},\, \ldots,\, c_{k_1}c_{k_2}\cdots c_{k_N})^T .
$$

In this case the truncated hierarchy can be written in vectorial form

$$
\partial_t \mathbf{u} + \partial_i \mathbf{F}^i(\mathbf{u}) = \mathbf{P}(\mathbf{u}),
\tag{3}
$$

where $\mathbf{u}$, $\mathbf{F}^i$, and $\mathbf{P}$ are, respectively the vectors of the densities, fluxes and productions terms:

$$
\mathbf{u} = \int mf\boldsymbol{\Phi}\, d\mathbf{c}, \qquad \mathbf{F}^i = \int mf\boldsymbol{\Phi}c_i\, d\mathbf{c}, \qquad \mathbf{P} = \int mQ\boldsymbol{\Phi}\, d\mathbf{c}.
\tag{4}
$$

When the system (3) is written explicitly, it is apparent that the well-known *problem of the closure* is faced: in order for the system to be closed, the flux of the last equation as well as the production terms must be assigned in RET as local function of the remaining moments appearing in the system:

$$
\begin{aligned}
&F_{k_1k_2\ldots k_Nk_{N+1}} \equiv F_{k_1k_2\ldots k_Nk_{N+1}}\left(F, F_{k_1}, F_{k_1k_2}, \ldots F_{k_1k_2\ldots k_N}\right), \\
&P_{k_1k_2\ldots k_j} \equiv P_{k_1k_2\ldots k_j}\left(F, F_{k_1}, F_{k_1k_2}, \ldots F_{k_1k_2\ldots k_n}\right), \quad 2 \leqslant j \leqslant N.
\end{aligned}
\tag{5}
$$

Since the equations of the hierarchy (3) are interpreted in RET as phenomenological equations of continuum mechanics, the original strategy for

solving the problem of the closure developed in RET consists in determining (5) by the exploitation of general principles of continuum physics, namely the entropy principle, the objectivity principle and the principle of thermodynamic stability [4, 5]. This strategy for the closure turns out to be powerful and leads in the 13 moment case ($N = 3$, considering only the trace of the last tensorial equation), at least not far from equilibrium, to the same closure as the strategy developed by Grad in the context of kinetic theory [6]. Unfortunately, it is difficult to apply the classical RET closure when the number of retained moments is large; in such cases an alternate procedure, based on another general physical principle – the Maximum Entropy Principle (MEP) – has been developed and successfully applied. When the MEP-based closure is exploited to close the system (3), the theory is referred to as Molecular Extended Thermodynamics (MET) [4].

According to the maximum entropy principle [8, 11, 12], the distribution function that describes in the best way the system (3) once the densities F, $F_{k_1}, \dots F_{k_1 k_2 \cdots k_N}$ are prescribed, named *distribution function of level N* [12], is the one that maximizes the entropy functional

$$h(f) = -k \int f \log\left(\frac{f}{y}\right) d\mathbf{c},$$

where k is the Boltzmann constant and y is a suitable factor necessary for dimensional reasons [4], under the constraint of given moments. Since the value of y only affects the additive constant appearing in the entropy, it is not essential and it is generally assumed without loss of generality to be unitary [5].

The distribution function of level N, denoted by f_N, is therefore found as the solution of the variational problem with constraints defined by the functional

$$\mathcal{L}_N(f) = -k \int f \log\left(\frac{f}{y}\right) d\mathbf{c} + \mathbf{u}' \cdot \left(\mathbf{F} - \int m f \boldsymbol{\Phi}\, d\mathbf{c}\right),$$

where $\mathbf{u}' = \left(u', u'_{k_1}, u'_{k_1} u'_{k_2}, \dots, u'_{k_1} u'_{k_2} \cdots u'_{k_N}\right)^T$ is the vector of the Lagrange multipliers. It is proven [8, 11] that the distribution function of level N, solution of the variational problem, is the following:

$$f_N = y \exp\left(-1 - \frac{m}{k}\chi_N\right), \quad \chi_N = \mathbf{u}' \cdot \boldsymbol{\Phi} = u' + \sum_{j=1}^{N} u'_{k_1 k_2 \dots k_j} c_{k_1} c_{k_2} \dots c_{k_j}. \quad (6)$$

If we insert (6) in the density vector $(4)_1$ we have a one-to-one map between the Lagrange multipliers and the densities; in this way we can express the Lagrange multipliers as functions of the field variables. Then, if we insert (6) in the last flux and in the productions $(4)_{2,3}$ we have an explicit expression for (5) and the system is closed. Moreover the Lagrange multipliers are coincident with the so called *main field* [19], which is the field that allows to write the system (3) in symmetric form [5, 8, 12, 20, 21]. The components of the main field vanish at equilibrium, except for the first components associated to the

conservation laws of Eq. (2) [12, 22]. At equilibrium, plugging the expressions of the non-vanishing components of the main field in Eq. (6), it is seen that the distribution function f_N coincides with the local Maxwellian distribution function [4]

$$f^{\mathcal{M}} = \frac{\rho}{m\left(2\pi p/\rho\right)^{3/2}} \exp\left(-\frac{\left(\mathbf{c}-\mathbf{v}\right)^2}{2p/\rho}\right), \tag{7}$$

where ρ, $\rho\mathbf{v}$, and p interpreted, respectively, as the mass, momentum, and pressure of the rarefied monatomic gas.

Unfortunately, the MEP-based procedure outlined above, despite its elegance and physically meaningful motivation, suffers from some serious issues that have hampered its application, at least in the classic formulation.

A remarkable restriction of its applicability consists in the fact that in order for the integrals to be convergent, the maximum rank N of the equations of the truncated system (3) must be even. Another issue with severe practical implications is that it is not possible, in general, to write the closing fluxes in closed-form, i.e. as functions of the remaining macroscopic quantities. Finally, it was shown [14, 23] that the domain of definition $\mathcal{U}$ of the flux of the last moment equation is not convex, the flux has a singularity, and the equilibrium state lies on the border of the domain of definition of the flux, $\partial\mathcal{U}$.

The key idea on which the application of the maximum entropy principle in RET relies on, consists in seeking a solution to the entropy maximization problem only near the local equilibrium. The distribution function f_N, given in Eq. (6), is thus formally expanded in the neighborhood of the equilibrium; the expansion up to an arbitrary order α reads [18]:

$$f_N^{(\alpha)} = f^{\mathcal{M}}\left(1+\sum_{h=1}^{\alpha}\frac{1}{h!}\left(-\frac{m}{k}\boldsymbol{\Lambda}\cdot\boldsymbol{\Phi}\right)^h\right), \qquad \boldsymbol{\Lambda} = \mathbf{u}' - \mathbf{u}'_E, \tag{8}$$

being $\boldsymbol{\Lambda}$ the non-equilibrium part of the Lagrange multipliers ($\mathbf{u}'_E$ is the vector of the Lagrange multipliers at equilibrium). In the context of MET, theories characterized by two different, in principle independent, orders of approximation can be formulated: the order N representing the maximum rank of the tensorial equations included in Eq. (3), and the order α appearing in Eq. (8) which represents the order of expansion about the equilibrium of the entropy-maximizing distribution function f_N. Such theories are denoted by ET_N^{α} [18].

In order to clarify the sequel, we now make a brief review of what has been shown first in the work of Brini and Ruggeri [18].

It is known [20] that, in order to ensure Galilean invariance, it exists an exponential matrix $\mathbf{X} \equiv \mathbf{X}(\mathbf{v})$, which becomes polynomial in the velocity components in the case of a system with the structure of Eq. (2), such that

$$\mathbf{u} = \mathbf{X}\hat{\mathbf{u}}, \qquad \mathbf{F}^i = \mathbf{X}\left(\hat{\mathbf{F}}^i + v_i\hat{\mathbf{u}}\right), \qquad \mathbf{P} = \mathbf{X}\hat{\mathbf{P}}, \qquad \mathbf{u}' = \hat{\mathbf{u}}'\mathbf{X}^{-1}, \tag{9}$$

where the quantities $\hat{\mathbf{u}}$, $\hat{\mathbf{F}}^i$, $\hat{\mathbf{P}}$, $\hat{\mathbf{u}}'$ are, respectively, the vectors of the densities, fluxes, production terms, and Lagrange multipliers (main field) evaluated for

$\mathbf{v} = 0$ (*intrinsic*, or *internal* quantities). It is convenient to compute the intrinsic closing fluxes and production terms, and then construct, when needed, the full moments by means of the relations given in Eq. (9). Introducing the peculiar velocity $\mathbf{C} = \mathbf{c} - \mathbf{v}$, and the vector $\hat{\boldsymbol{\Phi}}$ as

$$\hat{\boldsymbol{\Phi}} = (1,\, C_{k_1},\, C_{k_1}C_{k_2},\, \ldots,\, C_{k_1}C_{k_2}\cdots C_{k_N})^T\,,$$

where C_k $(k = 1, 2, 3)$ are the components of the peculiar velocity vector $\mathbf{C}$, we write

$$\hat{\mathbf{u}} = \int m f_N^{(\alpha)} \hat{\boldsymbol{\Phi}}\, d\mathbf{C}, \qquad \hat{\mathbf{u}}_E = \int m f^{\mathcal{M}} \hat{\boldsymbol{\Phi}}\, d\mathbf{C},$$

and the following vector is defined:

$$\Delta\hat{\mathbf{u}} = \hat{\mathbf{u}} - \hat{\mathbf{u}}_E = \int f^{\mathcal{M}} \sum_{h=1}^{\alpha} \frac{1}{h!} \left(-\frac{m}{k} \hat{\boldsymbol{\Lambda}} \cdot \hat{\boldsymbol{\Phi}}\right)^h \hat{\boldsymbol{\Phi}}\, d\mathbf{C}. \tag{10}$$

Denoting by $\hat{\boldsymbol{\Lambda}}^{(1)}$ and $\hat{\boldsymbol{\Lambda}}^{(2)}$, respectively, the first and second order terms of the non-equilibrium part of the intrinsic Lagrange multipliers $\left(\hat{\boldsymbol{\Lambda}} = \hat{\boldsymbol{\Lambda}}^{(1)} + \hat{\boldsymbol{\Lambda}}^{(2)} + \ldots\right)$, and taking into account that $\Delta\hat{\mathbf{u}}$ is, by definition, the vector of the non-equilibrium part of the field variables, we want to determine $\hat{\boldsymbol{\Lambda}}^{(1)}$ and $\hat{\boldsymbol{\Lambda}}^{(2)}$ as, respectively, first and second order polynomials in the components of $\Delta\hat{\mathbf{u}}$.

In the case of a second order expansion, we have from Eq. (10):

$$\Delta\hat{\mathbf{u}} = \int f^{\mathcal{M}} \left(-\frac{m}{k}\left(\hat{\boldsymbol{\Lambda}}^{(1)} + \hat{\boldsymbol{\Lambda}}^{(2)}\right) \cdot \hat{\boldsymbol{\Phi}} + \frac{1}{2}\left(\frac{m}{k}\left(\hat{\boldsymbol{\Lambda}}^{(1)} + \hat{\boldsymbol{\Lambda}}^{(2)}\right) \cdot \hat{\boldsymbol{\Phi}}\right)^2\right) \hat{\boldsymbol{\Phi}}\, d\mathbf{C}. \tag{11}$$

Retaining the first order terms in both members we have:

$$\Delta\hat{\mathbf{u}} = -\frac{m}{k} \int f^{\mathcal{M}} \left(\hat{\boldsymbol{\Lambda}}^{(1)} \cdot \hat{\boldsymbol{\Phi}}\right) \hat{\boldsymbol{\Phi}}\, d\mathbf{C}. \tag{12}$$

while at the second order we find, combining Eq. (11) and Eq. (12):

$$\mathbf{0} = \int f^{\mathcal{M}} \left(-\frac{m}{k}\left(\hat{\boldsymbol{\Lambda}}^{(2)} \cdot \hat{\boldsymbol{\Phi}}\right) + \frac{m^2}{2k^2}\left(\hat{\boldsymbol{\Lambda}}^{(1)} \cdot \hat{\boldsymbol{\Phi}}\right)^2\right) \boldsymbol{\Phi}\, d\mathbf{C}. \tag{13}$$

It has been noted [18] that Eq. (12) is a linear system in which the unknowns are the components of first order term of the non-equilibrium part of the intrinsic Lagrange multipliers, $\hat{\boldsymbol{\Lambda}}^{(1)}$. Once the linear system is solved, Eq. (13) is interpreted as a linear system for the components of $\hat{\boldsymbol{\Lambda}}^{(2)}$.

Either retaining only the first order term $(\hat{\boldsymbol{\Lambda}} = \hat{\boldsymbol{\Lambda}}^{(1)})$ or both the first and second order terms $(\hat{\boldsymbol{\Lambda}} = \hat{\boldsymbol{\Lambda}}^{(1)} + \hat{\boldsymbol{\Lambda}}^{(2)})$, once the quantities $\hat{\boldsymbol{\Lambda}}$ are obtained, the distribution function of level N is determined by Eq. (8) and the corresponding internal fluxes and internal productions are readily computed by means of Eq. $(4)_{2,3}$ evaluated at zero velocity:

$$\hat{\mathbf{F}}^{i(\alpha)} = \int m f_N^{(\alpha)} \hat{\boldsymbol{\Phi}}\, C_i\, d\mathbf{C}, \qquad \hat{\mathbf{P}} = \int m Q \hat{\boldsymbol{\Phi}}\, d\mathbf{C}. \tag{14}$$

Following [18] we can use the multi-index notation: C_A will indicate $C_{k_1}C_{k_2}\cdots C_{k_A}$, for $1 \leqslant A \leqslant N$ ($C_A = 1$ for $A = 0$). For other generic quantities, Ψ_A will indicate $\Psi_{k_1 k_2 \cdots k_A}$, for $1 \leqslant A \leqslant N$ ($\Psi_A = \Psi$ for $A = 0$). With this notation, the algebraic system (12) becomes:

$$\Delta \hat{u}_A = -\hat{\Lambda}^{(1)}_B \frac{m}{k} \int f^{\mathcal{M}} \hat{\Phi}_A \hat{\Phi}_B \, d\mathbf{C} = -\hat{\Lambda}^{(1)}_B I_{AB}, \tag{15}$$

where the integrals I_{AB}, being moments of the Maxwellian distribution function (7),

$$I_{AB} = \frac{m}{k} \int f^{\mathcal{M}} \hat{\Phi}_A \hat{\Phi}_B \, d\mathbf{C},$$

are completely known.

2.1 One-dimensional case

Focusing in the following on the one-dimensional case ($\mathbf{x} = (x_1, 0, 0)$, $\mathbf{v} = (v_1, 0, 0)$), these system (3) letting $x \equiv x_1$ and $\mathbf{F} = \mathbf{F}^1$ is written as

$$\partial_t \mathbf{u} + \partial_x \mathbf{F} = \mathbf{P}. \tag{16}$$

The procedure to compute the closing fluxes by means of the MEP can be broken down in following steps.

Step 1. In the one-dimensional case, only the first component C_1 of $\mathbf{C}$ or $C^2 = C_l C_l = C_1^2 + C_2^2 + C_3^2$ appears, and therefore it easy to see that the pair of multi-indexes (A, B) are mapped into the pair of indexes (r, s) such that

$$\hat{\Phi}_A = C_{k_1} C_{k_2} \ldots C_{k_A} \quad \longleftrightarrow \quad \hat{\Phi}_{rs} = C_1^r \left(C^2\right)^s.$$

The same correspondence exists between $I_{AB} \longleftrightarrow J_{rs}$ where

$$J_{rs} = \int m \, C_1^r \left(C^2\right)^s f^{\mathcal{M}} \, d\mathbf{C} = \begin{cases} 0 & r \text{ odd}, \\ \dfrac{1}{2^n} \left(\dfrac{2n+1}{r+1} \right) \dfrac{(2n)!}{n!} \dfrac{p^n}{\rho^{n-1}} & r \text{ even}, \end{cases}$$

being $n = r/2 + s$.

As a concrete example let consider for the 13 moment system in which

$$\mathbf{u} \equiv (F, F_1, F_{ll}, F_{<11>}, F_{ll1})^T \equiv (\rho, \rho v, \rho v^2 + 3p, \frac{2}{3}\rho v^2 - \sigma, 2q)^T \tag{17}$$

where ρ, v, p, σ, q are the mass density, the velocity, the pressure, the shear viscosity and the heat flux. Taking into account (17) and

$$\hat{\boldsymbol{\Phi}} \equiv \left(1, C_1, C^2, C_1^2 - \frac{1}{3}C^2, C^2 C_1\right)^T,$$

the linear system (15) becomes now

$$\begin{pmatrix} \Delta\hat{F} \\ \Delta\hat{F}_1 \\ \Delta\hat{F}_{kk} \\ \Delta\hat{F}_{\langle 11\rangle} \\ \Delta\hat{F}_{kk1} \end{pmatrix} = \begin{pmatrix} 0 \\ 0 \\ 0 \\ -\sigma \\ 2q \end{pmatrix} = -\mathbf{J} \begin{pmatrix} \hat{\Lambda}^{(1)} \\ \hat{\Lambda}^{(1)}_1 \\ \hat{\Lambda}^{(1)}_{kk} \\ \hat{\Lambda}^{(1)}_{\langle 11\rangle} \\ \hat{\Lambda}^{(1)}_{kk1} \end{pmatrix}. \tag{18}$$

The matrix $\mathbf{J}$ in this case can be written explicitly as

$$\begin{aligned} \mathbf{J} &\equiv \begin{pmatrix} J_{00} & J_{10} & J_{01} & J_{20} - \frac{1}{3}J_{01} & J_{11} \\ J_{10} & J_{20} & J_{11} & J_{30} - \frac{1}{3}J_{11} & J_{21} \\ J_{01} & J_{11} & J_{02} & J_{21} - \frac{1}{3}J_{02} & J_{12} \\ J_{20} - \frac{1}{3}J_{01} & J_{30} - \frac{1}{3}J_{11} & J_{01} & J_{40} - \frac{2}{3}J_{21} + \frac{1}{9}J_{02} & J_{31} - \frac{1}{3}J_{12} \\ J_{11} & J_{21} & J_{12} & J_{31} - \frac{1}{3}J_{12} & J_{22} \end{pmatrix} \\ &= \frac{m}{k} \begin{pmatrix} \rho & 0 & 3p & 0 & 0 \\ 0 & p & 0 & 0 & 5p^2/\rho \\ 3p & 0 & 15p^2/\rho & 0 & 0 \\ 0 & 0 & 0 & 4p^2/(3\rho) & 0 \\ 0 & 5p^2/\rho & 0 & 0 & 35p^3/\rho^2 \end{pmatrix}. \end{aligned} \tag{19}$$

Solving the linear system (18), it is found

$$\hat{\Lambda}^{(1)} = \hat{\Lambda}^{(1)}_{kk} = 0, \quad \hat{\Lambda}^{(1)}_1 = \frac{k}{m}\frac{\rho q}{p^2}, \quad \hat{\Lambda}^{(1)}_{\langle 11\rangle} = \frac{3}{4}\frac{k}{m}\frac{\rho\sigma}{p^2}, \quad \hat{\Lambda}^{(1)}_{kk1} = -\frac{1}{5}\frac{k}{m}\frac{\rho^2 q}{p^3}. \tag{20}$$

Step 2. Once the linear system is solved and the components of $\hat{\boldsymbol{\Lambda}}^{(1)}$ are known, the entropy-maximizing distribution function, $f_N^{(1)}$, is readily available:

$$f_N^{(1)} = f^{\mathcal{M}}\left(1 - \frac{m}{k}\hat{\boldsymbol{\Lambda}}^{(1)} \cdot \hat{\boldsymbol{\Phi}}\right),$$

which becomes, in the case of the one-dimensional 13 moment system the Grad one:

$$f_N^{(1)} = f^{\mathcal{M}}\left(1 - \frac{\rho q}{p^2}C_1 - \frac{3}{4}\frac{k}{m}\frac{\rho\sigma}{p^2}\left(C_1^2 - \frac{1}{3}C^2\right) + \frac{1}{5}\frac{k}{m}\frac{\rho^2 q}{p^3}C_1 C^2\right). \tag{21}$$

Step 3. The intrinsic fluxes resulting from a first order expansion ($\alpha = 1$) of the entropy-maximizing distribution, $f_N^{(1)}$, are now computed as follows (see Eq. (14)):

$$\hat{\mathbf{F}}^{(1)} = \int f^{\mathcal{M}}\left(1 - \frac{m}{k}\hat{\boldsymbol{\Lambda}}^{(1)} \cdot \hat{\boldsymbol{\Phi}}\right)\hat{\boldsymbol{\Phi}}\, C_1\, d\mathbf{C} = \int f_N^{(1)}\hat{\boldsymbol{\Phi}}\, C_1\, d\mathbf{C}.$$

Making use of Eq. (21), for the one-dimensional 13 moment system it is found

$$\hat{\mathbf{F}}^{(1)} = \left(0, \quad p - \sigma, \quad 2q, \quad \frac{8}{15}q, \quad 5\frac{p^2}{\rho} - 7\frac{p\sigma}{\rho}\right)^T. \tag{22}$$

Step 4. Proceeding further, Eq. (13) can be written as

$$0_D = \int f^{\mathcal{M}} \left(-\frac{m}{k} \hat{\Lambda}_A^{(2)} \hat{\Phi}_A + \frac{m^2}{2k^2} \hat{\Lambda}_A^{(1)} \hat{\Lambda}_B^{(1)} \hat{\Phi}_A \hat{\Phi}_B \right) \hat{\Phi}_D \, d\mathbf{C},$$

and we have the algebraic linear system for $\hat{\Lambda}_A^{(2)}$:

$$\hat{\Lambda}_A^{(1)} \hat{\Lambda}_D^{(1)} I_{ADB} = \hat{\Lambda}_A^{(2)} I_{AB}.$$

with

$$I_{ABD} = \frac{m^2}{2k^2} \int f^{\mathcal{M}} \hat{\Phi}_A \hat{\Phi}_B \hat{\Phi}_D \, d\mathbf{C}.$$

In the case of the one-dimensional I_{ABD} and I_{AB} can be mapped with J_{pr} and in particular in the case of 13 moment system, taking into account Eq. (19) and Eq. (20), we find

$$\begin{pmatrix} \frac{3}{8}\frac{\rho\sigma^2}{p^2} + \frac{1}{5}\frac{\rho^2 q^2}{p^3} \\ -\frac{2}{5}\frac{\rho\sigma q}{p^2} \\ \frac{21}{8}\frac{\sigma^2}{p} + \frac{9}{5}\frac{\rho q^2}{p^2} \\ \frac{1}{2}\frac{\sigma^2}{p} + \frac{12}{25}\frac{\rho q^2}{p^2} \\ -\frac{28}{5}\frac{\sigma q}{p} \end{pmatrix} = -\mathbf{J} \begin{pmatrix} \hat{\Lambda}^{(2)} \\ \hat{\Lambda}_1^{(2)} \\ \hat{\Lambda}_{kk}^{(2)} \\ \hat{\Lambda}_{\langle 11 \rangle}^{(2)} \\ \hat{\Lambda}_{kk1}^{(2)} \end{pmatrix}, \tag{23}$$

from which, by solving the linear system, we found:

$$\hat{\Lambda}^{(2)} = \frac{k}{m} \left(\frac{2}{5} \frac{\rho q^2}{p^3} - \frac{3}{8} \frac{\sigma^2}{p^2} \right), \qquad \hat{\Lambda}_1^{(2)} = \frac{7}{5} \frac{k}{m} \frac{\rho\sigma q}{p^3},$$
$$\hat{\Lambda}_{kk}^{(2)} = \frac{k}{m} \left(\frac{1}{5} \frac{\rho^2 q^2}{p^4} + \frac{1}{4} \frac{\rho\sigma^2}{p^3} \right), \qquad \hat{\Lambda}_{\langle 11 \rangle}^{(2)} = \frac{k}{m} \left(\frac{9}{25} \frac{\rho^2 q^2}{p^4} + \frac{3}{8} \frac{\rho\sigma^2}{p^3} \right),$$
$$\hat{\Lambda}_{kk1}^{(2)} = -\frac{9}{25} \frac{k}{m} \frac{\rho^2 \sigma q}{p^4}.$$

Step 5. Once the components of $\hat{\boldsymbol{\Lambda}}^{(2)}$ are known, the entropy-maximizing distribution function, $f_N^{(2)}$, is found as follows:

$$f_N^{(2)} = f^{\mathcal{M}} \left(1 - \frac{m}{k} \left(\hat{\boldsymbol{\Lambda}}^{(1)} + \hat{\boldsymbol{\Lambda}}^{(2)} \right) \cdot \hat{\boldsymbol{\Phi}} + \frac{m^2}{2k^2} \left(\hat{\boldsymbol{\Lambda}}^{(1)} \cdot \hat{\boldsymbol{\Phi}} \right)^2 \right).$$

For the one-dimensional 13 moment system, the previous expression can be written explicitly as follows:

$$
\begin{aligned}
f_N^{(2)} = f^{\mathcal{M}} \Bigg(& 1 + \frac{q^2\rho^4}{25p^6} C_1^2 C^4 + \frac{q\rho^3\sigma}{10p^5} C_1 C^4 + \frac{\rho^2\sigma^2}{16p^4} C^4 - \frac{3q\rho^3\sigma}{10p^5} C_1^3 C^2 + \\
& \left(\frac{3\rho^2\sigma^2}{8p^4} - \frac{2q^2\rho^3}{5p^5} \right) C_1^2 C^2 + \left(\frac{q\rho^2}{5p^3} - \frac{7q\rho^2\sigma}{50p^4} \right) C_1 C^2 + \\
& \left(\frac{\rho\sigma^2}{8p^3} + \frac{\rho\sigma}{4p^2} - \frac{2q^2\rho^2}{25p^4} \right) C^2 + \frac{9\rho^2\sigma^2}{16p^4} C_1^4 + \frac{3q\rho^2\sigma}{2p^4} C_1^3 + \\
& \left(\frac{16q^2\rho^2}{25p^4} - \frac{3\rho\sigma^2}{8p^3} - \frac{3\rho\sigma}{4p^2} \right) C_1^2 - \left(\frac{7q\rho\sigma}{5p^3} + \frac{q\rho}{p^2} \right) C_1 + \\
& \frac{2q^2\rho}{5p^3} + \frac{3\sigma^2}{8p^2} \Bigg) .
\end{aligned}
\tag{24}
$$

Step 6. The intrinsic fluxes resulting from a second order expansion ($\alpha = 2$) of the entropy-maximizing distribution function, $f_N^{(2)}$, are given by:

$$
\begin{aligned}
\hat{\mathbf{F}}^{(2)} &= \int f^{\mathcal{M}} \left(1 - \frac{m}{k} \left(\hat{\boldsymbol{\Lambda}}^{(1)} + \hat{\boldsymbol{\Lambda}}^{(2)} \right) \cdot \hat{\boldsymbol{\Phi}} + \frac{m^2}{2k^2} \left(\hat{\boldsymbol{\Lambda}}^{(1)} \cdot \hat{\boldsymbol{\Phi}} \right)^2 \right) \hat{\boldsymbol{\Phi}} \, C_i \, d\mathbf{C} \\
&= \int f_N^{(2)} \hat{\boldsymbol{\Phi}} \, C_1 \, d\mathbf{C}.
\end{aligned}
$$

Making use of Eq. (24) and recalling Eq. (22) , it is found after lengthy calculations:

$$
\hat{\mathbf{F}}^{(2)} = \hat{\mathbf{F}}^{(1)} + \left(0, \quad 0, \quad 0, \quad -\frac{36}{25} \frac{\sigma q}{p}, \quad \frac{148}{25} \frac{q^2}{p} + 2\frac{\sigma^2}{\rho} \right)^T . \tag{25}
$$

This procedure was given for 13 moments also in 3-dimensional case by Brini and Ruggeri [16].

Further steps. Even though in the sequel we shall not consider expansions beyond the second order, we note that the procedure outlined above is generalized to any order of expansion α as follows: Once the components of $\hat{\boldsymbol{\Lambda}}^{(1)}$, $\hat{\boldsymbol{\Lambda}}^{(2)}$, $\dots \hat{\boldsymbol{\Lambda}}^{(\alpha-1)}$ are known, the components of the α order term, $\hat{\boldsymbol{\Lambda}}^{(\alpha)}$, are found solving the linear system

$$
I_{AB} \hat{\Lambda}_A^{(\alpha)} = \sum_{h=1}^{\alpha} \frac{1}{h!} \left(\frac{-1}{k} \right)^h \left(\sum_{\substack{\beta_1, \beta_2, \dots \beta_h = 1 \\ \beta_1 + \beta_2 + \dots + \beta_h = \alpha \\ \beta_1 \leqslant \beta_2 \leqslant \dots \leqslant \beta_h}}^{\alpha - h + 1} \hat{\Lambda}_{A_1}^{(\beta_1)} \hat{\Lambda}_{A_2}^{(\beta_2)} \cdots \hat{\Lambda}_{A_h}^{(\beta_h)} I_{A_1 A_2 \dots A_h B} \right) ,
$$

where

$$
I_{A_1 A_2 \dots A_a B} = \int f^{\mathcal{M}} \hat{\Phi}_{A_1} \hat{\Phi}_{A_2} \cdots \hat{\Phi}_{A_a} \hat{\Phi}_B \, d\mathbf{C}
$$

and, following the procedure outlined above, $I_{A_1A_2\ldots A_aB}$ can be mapped to the matrix J_{pq}. At each iteration of the procedure, a linear system similar similar to those of Eq. (18) and Eq. (23) are found. All these linear systems are characterized by the same matrix $\mathbf{J}$ given in (19) and they differ only for the terms appearing on the left-hand side in Eq. (18) and Eq. (23).

3 Moment System of a Monatomic Gas: $\mathbf{ET^1_{13}}$ and $\mathbf{ET^2_{13}}$

Taking into account that in the case of 13 moments in one-dimensional case the matrix $\mathbf{X}$ is given by [20]

$$\mathbf{X} = \begin{pmatrix} 1 & 0 & 0 & 0 & 0 \\ v & 1 & 0 & 0 & 0 \\ v^2 & 2v & 1 & 0 & 0 \\ \frac{2}{3}v^2 & \frac{4}{3}v & 0 & 1 & 0 \\ v^3 & 3v^2 & \frac{5}{3}v & 2v & 1 \end{pmatrix},$$

we can obtain using (9) the field, the total flux and productions at first and second order:

$$\mathbf{u} = \begin{pmatrix} F \\ F_1 \\ F_{kk} \\ F_{\langle 11\rangle} \\ F_{kk1} \end{pmatrix} = \begin{pmatrix} \rho \\ \rho v \\ \rho v^2 + 3p \\ \frac{2}{3}\rho v^2 - \sigma \\ \rho v^3 + 5pv - 2\sigma v + 2q \end{pmatrix}, \qquad \mathbf{P} = \begin{pmatrix} 0 \\ 0 \\ 0 \\ P_{\langle 11\rangle} \\ P_{kk1} \end{pmatrix}, \tag{26}$$

$$\mathbf{F}^{(1)} = \begin{pmatrix} F^{(1)}_1 \\ F^{(1)}_{11} \\ F^{(1)}_{kk1} \\ F^{(1)}_{\langle 11\rangle 1} \\ F^{(1)}_{kk11} \end{pmatrix} = \begin{pmatrix} \rho v \\ \rho v^2 + p - \sigma \\ \rho v^3 + 5pv - 2\sigma v + 2q \\ \frac{2}{3}\rho v^3 + \frac{4}{3}pv - \frac{7}{3}\sigma v + \frac{8}{15}q \\ \rho v^4 + (8p - 5\sigma)\, v^2 + \frac{32}{5}qv + 5\frac{p^2}{\rho} - 7\frac{p\sigma}{\rho} \end{pmatrix}. \tag{27}$$

$$\mathbf{F}^{(2)} = \begin{pmatrix} F^{(2)}_1 \\ F^{(2)}_{11} \\ F^{(2)}_{kk1} \\ F^{(2)}_{\langle 11\rangle 1} \\ F^{(2)}_{kk11} \end{pmatrix} = \begin{pmatrix} \rho v \\ \rho v^2 + p - \sigma \\ \rho v^3 + 5pv - 2\sigma v + 2q \\ \frac{2}{3}\rho v^3 + \frac{4}{3}pv - \frac{7}{3}\sigma v + \frac{8}{15}q - \frac{36}{25p}\sigma q \\ \rho v^4 + (8p - 5\sigma)\, v^2 + \frac{32}{5}qv + 5\frac{p^2}{\rho} - 7\frac{p\sigma}{\rho} + 2\frac{\sigma^2}{\rho} + \frac{148}{25}\frac{q^2}{p}. \end{pmatrix}. \tag{28}$$

The non-zero components of the production term $\mathbf{P}$ are here assumed to be given by the following expressions [5]:

$$P_{\langle 11\rangle} = \frac{\sigma}{\tau_\sigma}, \qquad P_{kk1} = \frac{2\sigma v}{\tau_\sigma} - \frac{2q}{\tau_q}.$$

The coefficients τ_σ and τ_q are relaxation times associated, respectively, to non-equilibrium processes connected to the viscosity and heat conductivity of the gas. In the following, in view of comparing the results obtained by solving the moment equations with those obtained by solving the Boltzmann equation with the BGK approximation for the collision term (which involves one single relaxation time), we shall assume that these relaxation times are equal: $\tau = \tau_\sigma = \tau_q$, such that

$$P_{\langle 11\rangle} = \frac{\sigma}{\tau}, \qquad P_{kk1} = \frac{2\left(\sigma v - q\right)}{\tau}. \tag{29}$$

Inserting (26), (27) and (29) in the system (16) we have the closed system at first order, while if we insert as flux (28) we have the closure at second order. The three-dimensional case was obtained in [16].

4 Shock Structure Solution

A *shock structure solution* of the one-dimensional system given in Eq. (16) is a continuous solution of the form

$$\mathbf{u} = \mathbf{u}\left(\varphi\right), \qquad \varphi = x - st,$$

such that

$$\lim_{\varphi\to-\infty} \mathbf{u}\left(\varphi\right) = \mathbf{u}_1, \qquad \lim_{\varphi\to+\infty} \mathbf{u}\left(\varphi\right) = \mathbf{u}_0, \qquad \lim_{\varphi\to\pm\infty} \frac{d\mathbf{u}}{d\varphi} = 0,$$

where $\mathbf{u}_0$, $\mathbf{u}_1$ are equilibrium states and s is the *speed* of the traveling wave. Assuming, without loss of generality, that $s > 0$, the states $\mathbf{u}_0$ and $\mathbf{u}_1$ are denoted, respectively, as *unperturbed* and *perturbed* states.

Writing the system (16) in the form

$$\partial_t \mathbf{u} + \mathbf{A}\left(\mathbf{u}\right)\partial_x \mathbf{u} = \mathbf{P}\left(\mathbf{u}\right), \qquad \mathbf{A} = \nabla_{\mathbf{u}}\mathbf{F},$$

where $\mathbf{A}$ is the Jacobian of the flux $\mathbf{F}$ with respect to the field variables $\mathbf{u}$, it is seen [15] that a shock structure solution satisfies

$$\frac{d}{d\varphi}\left(-s\mathbf{u} + \mathbf{F}\right) = \mathbf{P}\left(\mathbf{u}\right),$$

or, equivalently,

$$\left(-s\mathbf{I} + \mathbf{A}\left(\mathbf{u}\right)\right)\frac{d\mathbf{u}}{d\varphi} = \mathbf{P}\left(\mathbf{u}\right). \tag{30}$$

The shock speed s is often replaced by the so-called Mach number which, evaluated in the unperturbed state $\mathbf{u}_0$, is defined as $M_0 = \left(s - v_0\right)/c_0$, where v_0 and c_0 are, respectively, the gas velocity and the sound velocity in the state $\mathbf{u}_0$ (in general, here and in the following the subscripts "0" and "1" denote a quantity evaluated, respectively, in the unperturbed and perturbed state).

The integration of the first three scalar equations of the system (30), representing the conservation laws of mass, momentum and energy, leads to the following relations between the two equilibrium states $\mathbf{u}_0$ and $\mathbf{u}_1$, i.e. the Rankine-Hugoniot compatibility conditions of the equilibrium subsystem [24]:

$$\frac{\rho_1}{\rho_0} = \frac{4M_0^2}{M_0^2+3}, \qquad \frac{u_1}{u_0} = \frac{M_0^2+3}{4M_0^2}, \qquad \frac{p_1}{p_0} = \frac{5M_0^2-1}{4},$$

where, having introduced the relative velocity $u = v - s$, the quantities ρ_0, $u_0 = v_0 - s$, p_0 and ρ_1, $u_1 = v_1 - s$, p_1 are the density, relative velocity and pressure of, respectively, the unperturbed and perturbed states.

4.1 Shock Structure in ET_{13}^1

Introducing the following non-dimensional variables:

$$\hat{\varphi} = \frac{\varphi}{\tau c_0}, \qquad \hat{\rho} = \frac{\rho}{\rho_0}, \qquad \hat{u} = \frac{u}{c_0} = -M_0\frac{u}{u_0},$$
$$\hat{p} = \frac{p}{p_0}, \qquad \hat{\sigma} = \frac{\sigma}{p_0}, \qquad \hat{q} = \frac{q}{p_0 c_0},$$

the system of ordinary differential equations given in Eq. (30) with the flux $\mathbf{F}$ obtained by means of the first order closure i.e. with the closing fluxes given by Eq. (27), is written in non-dimensional form after suitable manipulation as

$$\begin{aligned}
&\rho = -M_0/u,\\
&\sigma = -\frac{5}{3}M_0^2 - \frac{5}{3}M_0 u + p - 1,\\
&q = \frac{1}{2}\left(-\frac{5}{3}M_0^3 - \frac{10}{3}M_0^2 u - \frac{5}{3}M_0 u^2 - 5M_0 - 3pu - 2u\right),\\
&\frac{d}{d\varphi}\left(4M_0^3 - 27M_0^2 u - 21M_0 u^2 + 12M_0 + \frac{81pu}{5} - \frac{81u}{5}\right) =\\
&\qquad\qquad 15M_0\left(M_0 - u\right) - 9\left(p-1\right),\\
&\frac{d}{d\varphi}\Big(\frac{u}{25}\left(-80M_0^4 - 35M_0^3 u - 105M_0^2 p + 20M_0^2 u^2 - 240M_0^2 - 204M_0 pu\right.\\
&\qquad\left.-21M_0 u + 18p^2 - 63p\right)\Big) = M_0\left(M_0^3 - M_0 u^2 + 3M_0 + 3pu\right),
\end{aligned} \tag{31}$$

where the "hat" symbol on the quantities φ, ρ, u, p, σ, q was dropped for ease of notation and the unperturbed Mach number M_0 was used in place of the shock speed s.

4.2 Shock Structure in ET_{13}^{2}

When the flux $\mathbf{F}$ is obtained by means of the second order closure i.e. making use of the closing fluxes given by Eq. (28), the system of ordinary differential equations in Eq. (30), written in non-dimensional form, becomes:

$$
\begin{aligned}
&\rho = -M_0/u,\\
&\sigma = -\frac{5}{3}M_0^2 - \frac{5}{3}M_0 u + p - 1,\\
&q = \frac{1}{2}\left(-\frac{5}{3}M_0^3 - \frac{10}{3}M_0^2 u - \frac{5}{3}M_0 u^2 - 5M_0 - 3pu - 2u\right),\\
&\frac{d}{d\varphi}\left(\frac{1}{25p}\left(-450M_0^5 - 1350M_0^4 u + 170M_0^3 p - 1350M_0^3 u^2 - 1620M_0^3 + \right.\right.\\
&\quad 405M_0^2 pu - 450M_0^2 u^3 - 2430M_0^2 u - 15M_0 pu^2 + 510M_0 p - 810M_0 u^2,\\
&\quad \left.\left. -810M_0 + 81p^2 u + 243pu - 324u\right)\right) = 15M_0\left(M_0 - u\right) - 9\left(p - 1\right),\\
&\frac{d}{d\varphi}\left(\frac{1}{15p}\left(925M_0^7 + 2800M_0^6 u + 2850M_0^5 u^2 + 5550M_0^5 + 1920M_0^4 pu + 1000M_0^4 u^3 + \right.\right.\\
&\quad 10080M_0^4 u + 4095M_0^3 pu^2 + 25M_0^3 u^4 + 5130M_0^3 u^2 + 8325M_0^3 -\\
&\quad 675M_0^2 p^2 u + 1800M_0^2 pu^3 + 7110M_0^2 pu + 600M_0^2 u^3 + 5040M_0^2 u +\\
&\quad \left.\left. 1809M_0 p^2 u^2 + 2457M_0 pu^2 + 684M_0 u^2 - 405p^2 u - 270pu\right)\right) =\\
&\qquad M_0\left(M_0^3 - M_0 u^2 + 3M_0 + 3pu\right),
\end{aligned}
\tag{32}
$$

where, as before, the "hat" symbol was dropped.

5 Shock Structure Solution with Subshock

Denoting with $\lambda_0^{(max)}$ the maximum characteristic speed (i.e. the largest eigenvalue of the matrix $\mathbf{A}$) in the unperturbed state $\mathbf{u}_0$, it was proven that when $s > \lambda_0^{(max)}$, or equivalently when $M_0 > \left(\lambda_0^{(max)} - v_0\right)/c_0$, no continuous shock structure solution exists [15]. In this case, the solution develops a discontinuity known as *subshock*.

The study of the subshock features is based on the Rankine-Hugoniot compatibility conditions that must hold across the subshock front:

$$
-s\left[\!\left[\mathbf{u}\right]\!\right]_* + \left[\!\left[\mathbf{F}(\mathbf{u})\right]\!\right]_* = 0, \tag{33}
$$

where $\left[\!\left[\psi\right]\!\right]_* = \psi_* - \psi_0$ represents the *jump* across the discontinuity (subshock) of the generic quantity ψ (ψ_* and ψ_0 denote, respectively, the values of the quantity ψ evaluated in the perturbed state $\mathbf{u}_*$ behind the subshock and in the unperturbed state $\mathbf{u}_0$ after the subshock).

According to the general theory of hyperbolic systems, shocks are one-parameter families of solutions corresponding to the bifurcated branches of the

trivial solution (null shock) obtained when the shock parameter s approaches a characteristic velocity of the system. It is known that, for the Grad system of Eq. (16), when the shock front is propagating in an equilibrium state $\mathbf{u}_0$, the null shock is generated when the Mach number in the unperturbed state, M_0, is a root of the bi-quadratic polynomial equation $25M_0^4 - 78M_0^2 + 27 = 0$, i.e. $M_0 = \mp\frac{1}{5}\sqrt{3\left(13-\sqrt{94}\right)} \simeq \mp 0.63$ or $M_0 = \mp\frac{1}{5}\sqrt{3\left(13+\sqrt{94}\right)} \simeq \mp 1.65$. In particular, it is seen that when $M_0 \gtrsim 1.65 = M_0^{cr}$ (the largest root of the bi-quadratic polynomial equation), the so-called *fast shock* appears.

5.1 First Order Closure

The main features of the solution of the system of non-linear equations given in Eq. (33) for the 13 moment system when a first order closure is exploited, i.e. when the closing fluxes are those given in Eq. (22), were studied in [4,25]. In this case, the Rankine-Hugoniot compatibility conditions (33) provide

$$\begin{aligned}
&[\![\rho u]\!]_* = 0,\\
&[\![\rho u^2 + p - \sigma]\!]_* = 0,\\
&[\![\rho u^3 + 5pu - 2\sigma u + 2q]\!]_* = 0,\\
&\left[\!\!\left[\frac{2}{3}\rho u^3 + \frac{4}{3}pu - \frac{7}{3}\sigma u + \frac{8}{15}q\right]\!\!\right]_* = 0,\\
&\left[\!\!\left[\rho u^4 + (8p - 5\sigma)\,u^2 + \frac{16}{3}qu + \frac{16}{15}qu + 5\frac{p^2}{\rho} - 7\frac{p\sigma}{\rho}\right]\!\!\right]_* = 0.
\end{aligned} \tag{34}$$

In [25] it was found that the admissible fast shock bifurcating from the null shock corresponding to $M_0 \simeq 1.65$ is compressive and the ratio of the mass density ahead and behind the shock, $w = \rho_0/\rho_*$ (compression factor), is monotonously decreasing as the Mach number M_0 increases beyond the critical value $M_0 \simeq 1.65$. It was also proved the existence of a lower bound $w_{cr} \simeq 0.71$ for the compression factor w, as shown in Fig. 1, and it was argued that the characteristic velocities of the system along the non-equilibrium process across the shock front are all real as long as $M_0 \lesssim 2.7$, while for larger values of the Mach number M_0 the process exits the hyperbolicity region. This property of the system is depicted in Fig. 2, where it is shown that for $M_0 \simeq 2.7$ a bifurcation of the real part of the two minimum eigenvalues (evaluated in the perturbed state $\mathbf{u}_*$ behind the subshock) of the system occurs. This is an indicator of the fact that the two characteristic velocities become complex conjugates for $M_0 \gtrsim 2.7$.

5.2 Second Order Closure

When the second order closure is exploited, i.e. when the closing fluxes are those given in Eq. (25), the Rankine-Hugoniot conditions across the subshock

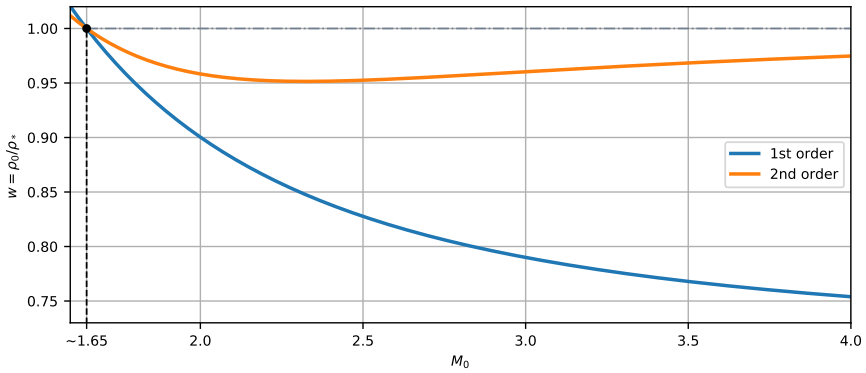

Fig. 1 Compression factor w, i.e. ratio of the mass density ahead and behind the fast subshock front ($w = \rho_0/\rho_*$), predicted for the 13-moment system for a monatomic gas with first and second order maximum entropy principle closure (respectively, blue curve and orange curve), as a function of the unperturbed Mach number M_0.

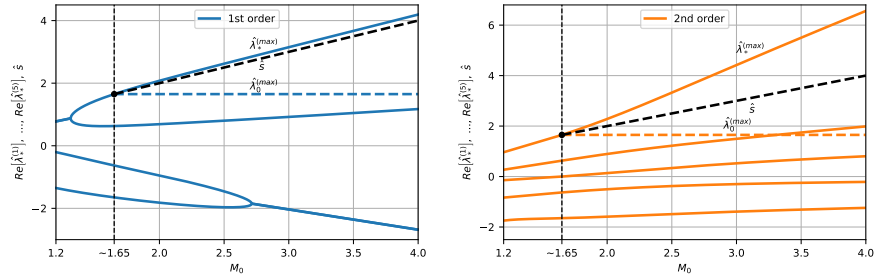

Fig. 2 Real part of the dimensionless characteristic velocities $\hat{\lambda}_*^{(k)}$ $(k = 1, \dots 5)$ evaluated in the state $\mathbf{u}_*$ behind the shock, predicted by the 13-Moment system for a monatomic gas with first order (on the left) and second order (on the right) maximum entropy principle closures, as a function of the unperturbed Mach number M_0. The dashed lines represent the maximum characteristic speed in the unperturbed state, $\hat{\lambda}_0^{(max)}$, and the dimensionless shock speed, $\hat{s}$. The dashed lines are plotted to show graphically that the Lax admissibility condition holds, i.e. $\hat{\lambda}_0^{(max)} < \hat{s} < \hat{\lambda}_*^{(max)}$, when $M_0 \gtrsim 1.65$.

front, Eq. (33), are written as

$$
\begin{aligned}
&[\![\rho u]\!]_* = 0,\\
&[\![\rho u^2 + p - \sigma]\!]_* = 0,\\
&[\![\rho u^3 + 5pu - 2\sigma u + 2q]\!]_* = 0,\\
&\left[\!\!\left[\frac{2}{3}\rho u^3 + \frac{4}{3}pu - \frac{7}{3}\sigma u + \frac{8}{15}q - \frac{36}{25}\frac{\sigma q}{p}\right]\!\!\right]_* = 0,\\
&\left[\!\!\left[\rho u^4 + (8p - 5\sigma)\,u^2 + \frac{16}{3}qu + 2\left(\frac{8}{15}q - \frac{36}{25}\frac{\sigma q}{p}\right)u + 5\frac{p^2}{\rho} - 7\frac{p\sigma}{\rho} + \right.\right.\\
&\qquad\left.\left. 2\frac{\sigma^2}{\rho} + \frac{148}{25}\frac{q^2}{p}\right]\!\!\right]_* = 0.
\end{aligned}
\tag{35}
$$

It is found that the solution of the non-linear system (35) is qualitatively different from the solution of the system obtained with the first order closure, represented in Eq. (34). A remarkable result is the following. The compression factor w as a function of the Mach number M_0, when the second order closure in exploited, is not monotonously decreasing as in the case of the first order closure. Indeed, a numerical solution of the system in Eq. (35) shows that the ratio of the mass density, $w = \rho_0/\rho_*$, decreases for increasing values of the unperturbed Mach number in the interval $1.65 \lesssim M_0 \lesssim 2.3$, reaching a minimum value $w_{min} \simeq 0.951$, and then increases monotonously towards the asymptotic value $w = 1$ for larger values of the unperturbed Mach number ($M_0 \gtrsim 2.3$). In Fig. 1, this behavior is compared to the monotonously decreasing behavior of the compression factor w found with the traditional first order closure [25].

The prediction of the compression factor w found with the second order closure should be regarded as an improvement over the prediction provided by the first order closure, since it suggests that when a second order closure is adopted, the strength of the subshock appearing in the solution is in general reduced, thus leading to a shock profile that, as long as the unrealistic discontinuity is concerned, might be closer to the shock profile observed experimentally, and theoretically obtained by means of the kinetic model based on the Boltzmann equation, where no discontinuous shock profile is ever observed. This expectation is confirmed by numerically solving for several values of the unperturbed Mach number M_0 the systems in Eq. (31) and in Eq. (32) providing the shock structure solution for a monatomic gas modeled by means of the 13 moment system with first and second order closures. A selection of these results is presented in Section 6.

It is also remarkable that the characteristic velocities of the system in the state $\mathbf{u}_*$ behind the subshock front are found to be real also for values beyond the limit value of the unperturbed Mach number found in the case of the first oder closure, i.e. $M_0 \simeq 2.7$ (see Fig. 2). It was observed by means of numerical computations that in the framework of the 13 moment system of a monatomic gas with a second order closure, the hyperbolicity region is never abandoned along the whole non-equilibrium process across the shock structure, at least for values of the unperturbed Mach number M_0 up to 4. This interesting feature is possible due to the peculiar topology of the hyperbolicity region discussed in [16]: Even for *large* value of the Mach number M_0, that lead to a shock profile characterized by strong departures from the equilibrium along the shock process, the non-equilibrium states in which the system is found are always inside the hyperbolicity region marked as "Region I" recently discussed by Brini and Ruggeri (see Section 5 and in particular Figure 2 in [16]).

6 Numerical results

In order to investigate the properties of the shock structure solution with and without subshock obtained for the 13 moment system with first and second order MEP closures, the systems of ordinary differential equations given in

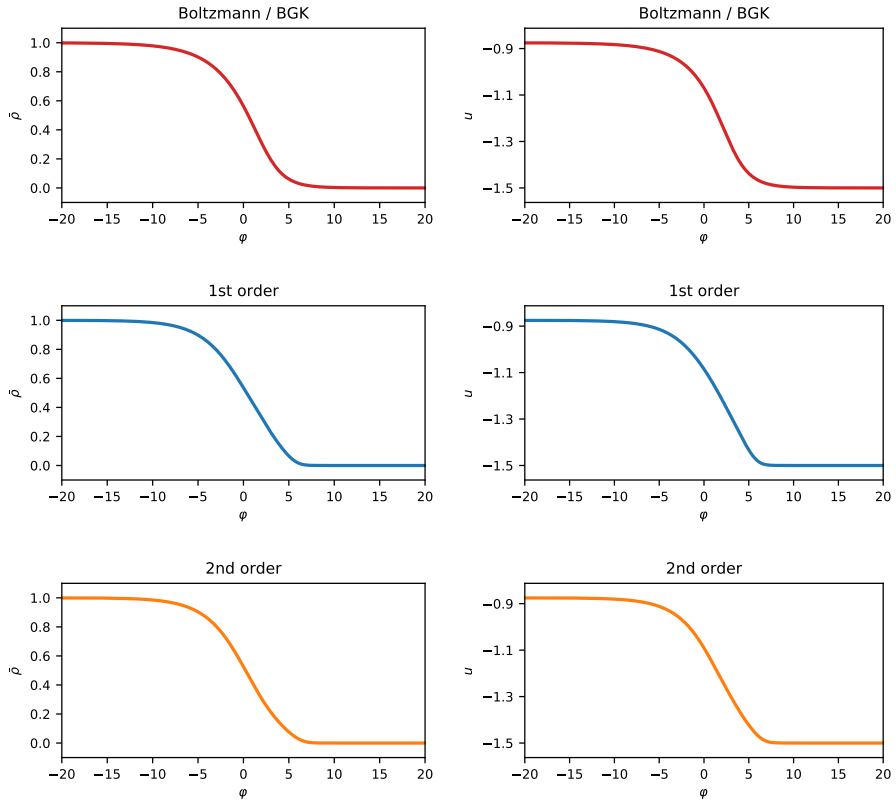

Fig. 3 Rescaled mass density profile $\bar{\rho} = (\rho - \rho_0)/(\rho_1 - \rho_0)$ (on the left) and relative velocity profile $u = v - s$ (on the right) of the shock structure solution obtained for $M_0 = 1.5$ in a monatomic gas with the Boltzmann/BGK model (top row), and with the 13 moment system with the first order MEP closure (middle row) and second order MEP closure (bottom row).

Eq. (31) and Eq. (32) are numerically solved for different values of the shock parameter, i.e. the unperturbed Mach number M_0.

In addition, the numerical solutions of Eq. (31) and Eq. (32) are compared to the numerical solution of the Boltzmann equation with the BGK approximation for the collision term. The Boltzmann/BGK model equation (1), written for the one-dimensional case, reads as follows:

$$\partial_t f + c_1\, \partial_x f = -\frac{f - f^{\mathcal{M}}}{\tau}, \tag{36}$$

where $f \equiv f\left(x, c_1, c^2, t\right)$ and $f^{\mathcal{M}}$ is the local Maxwellian equilibrium distribution given in Eq. (7), and the relaxation time τ is the same parameter appearing in the production terms given in Eq. (29). We stress here that in order for such a comparison to be consistent, since the Boltzmann/BGK model involves one single relaxation time τ, the relaxation times associated to the viscosity

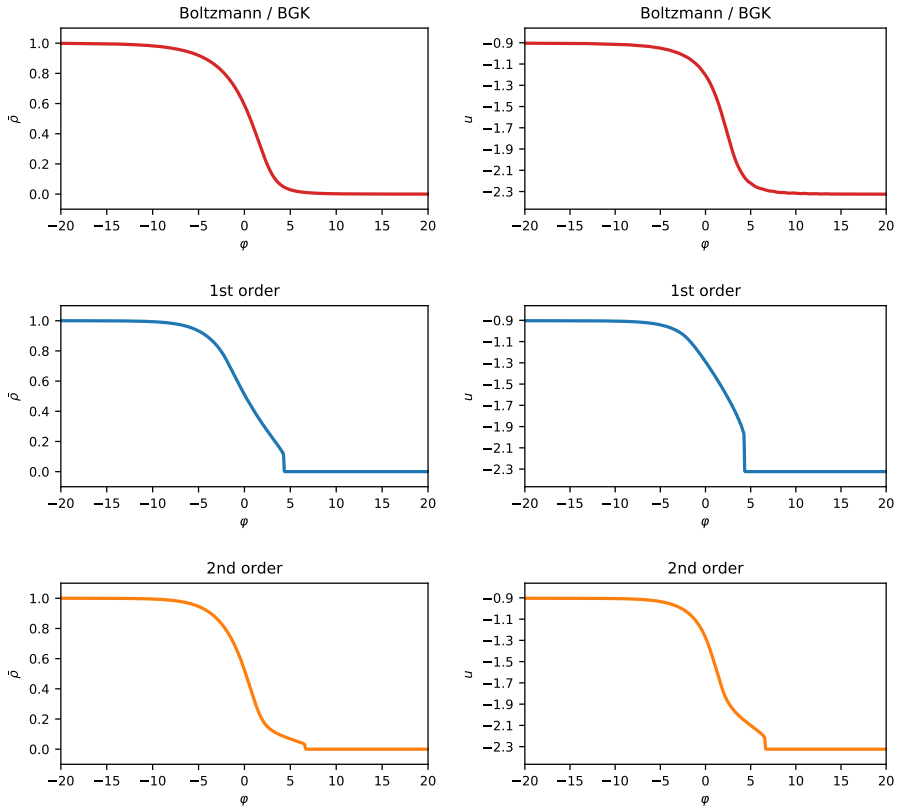

Fig. 4 Rescaled mass density profile $\bar{\rho} = (\rho - \rho_0)/(\rho_1 - \rho_0)$ (on the left) and relative velocity profile $u = v - s$ (on the right) of the shock structure solution obtained for $M_0 = 2.3$ in a monatomic gas with the Boltzmann/BGK model (top row), and with the 13 moment system with the first order MEP closure (middle row) and second order MEP closure (bottom row).

and heat conductivity appearing in the 13 moment system are assumed to be equal ($\tau = \tau_\sigma = \tau_q$).

The details of the numerical techniques used to solve the moment equations as well as the Boltzmann/BGK equation are illustrated in a paper under preparation. In this section, a selection of the numerical results is presented as to show the impact of the chosen order of the closure (either first, or second) on the obtained shock structure profiles, and to compare these profiles to the reference solution obtained solving the Boltzmann/BGK equation given in Eq. (36). To this aim, in the following the density and velocity profiles across the shock structure obtained with the Boltzmann/BGK model and with the 13 moment system with first and second order closures for $M_0 = 1.5,\ 2.3,\ 4$ are reported.

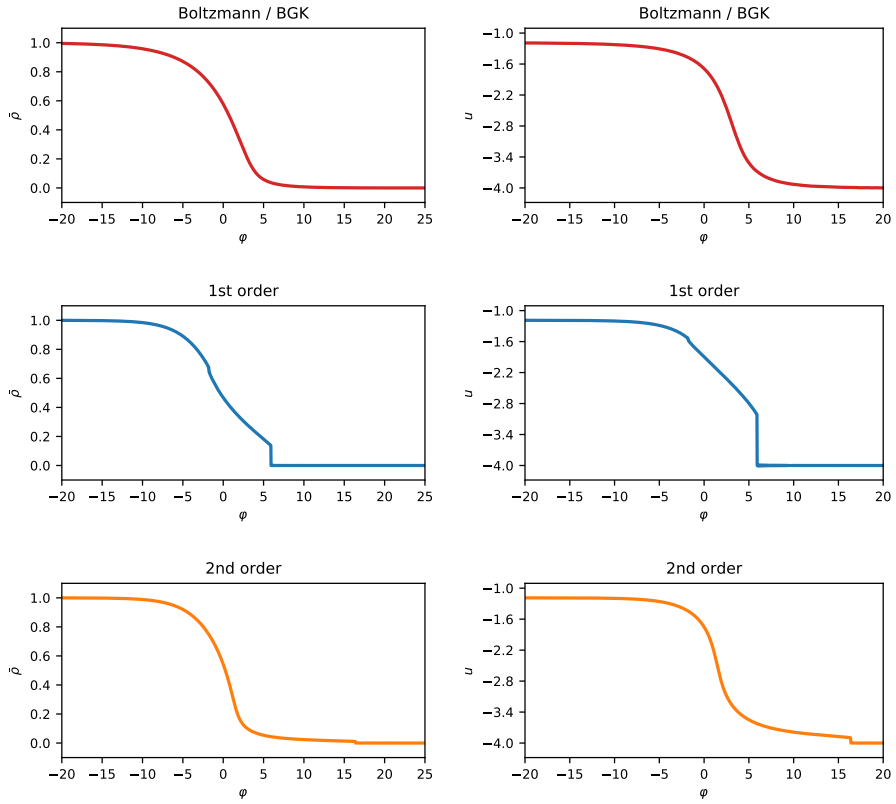

Fig. 5 Rescaled mass density profile $\bar{\rho} = (\rho - \rho_0)/(\rho_1 - \rho_0)$ (on the left) and relative velocity profile $u = v - s$ (on the right) of the shock structure solution obtained for $M_0 = 4.0$ in a monatomic gas with the Boltzmann/BGK model (top row), and with the 13 moment system with the first order MEP closure (middle row) and second order MEP closure (bottom row).

In Fig. 3, the case of the shock structure obtained with $M_0 = 1.5$ is presented. In agreement with the expectations [12, 24], in this case the shock structure profile is continuous, namely it does not present any discontinuity connected with a subshock formation, being the unperturbed Mach number M_0 less than the critical value $M_0^{cr} \simeq 1.65$. The results obtained in the framework of the 13 moment theory by means of a first order closure present a smooth but somewhat rapid transition from the unperturbed field to the perturbed one in the foremost part of the shock profile. Such a sharp (but continuous) transition is smoothed out when the second order closure is adopted, leading to a shock profile which looks arguably closer to the reference solution obtained making use of the kinetic model equation.

In Fig. 4, the case of the shock structure obtained with $M_0 = 2.3$ is reported. In this case, the profile of the shock structure includes a discontinuity,

i.e. a subshock, when the traditional first order closure of the 13 moment system is adopted. This is predicted by the theory, since in this case the unperturbed Mach number M_0 exceeds the critical value given by the largest characteristic velocity in the unperturbed state ($M_0^{cr} \simeq 1.65$). The subshock formation is also evident in the shock structure profile obtained with a second order closure, but in this case the profile is overall qualitatively different from the one obtained with the linear closure. In particular, it is seen that the *strength* of the subshock, i.e. the jump in the field variables across the subshock front is smaller than the one found by making use of the linear closure. This is in agreement with the theoretical results illustrated in Section 5, in particular with the behavior found for the compression factor $w = \rho_0/\rho_*$ as a function of the unperturbed Mach number (see Fig. 1), which predicts for $M_0 = 2.3$ a compression factor close to unity ($w \simeq 0.954$), and therefore a *small* jump in the density profile. This prediction is consistent with the numerical results shown in Fig. 4.

Despite the fact that the overall shock structure profile is not matching particularly well the reference results obtained in the framework of the kinetic model, it is safe to say that the formation of the unphysical subshock discontinuity is a less prominent feature of the shock structure solution when the quadratic closure is adopted, in comparison to the solution obtained with the linear closure.

It is worth noticing that the subshock formation, which takes place when the speed s of the shock front exceeds the maximum characteristic velocity of the system evaluated in the unperturbed state [12] is independent from the chosen order of the closure. This is due to the fact that, being the unperturbed state an equilibrium state, the fluxes of the moment equations are clearly independent from the chosen closure in any equilibrium state. As a consequence, the formation of a subshock is expected to be found independently from the order of the closure (first, second, or even higher); the strength of the subshock, in contrast, strongly depends on the non-equilibrium fluxes, and hence on the adopted closure.

The case of a shock structure profile with $M_0 = 4$ is presented in Fig. 5. As predicted by the theory, the shock profile obtained with the first order closure is affected by a rather pronounced unphysical jump in the foremost part of the shock profile, leading to a solution that remarkably differentiates from the one obtained with the kinetic model. Inspection of the density and velocity profiles reported in Fig. 5 suggests that in this case there is even the onset of a second subshock which propagates in the perturbed state behind the first (most noticeable) subshock.

Interestingly, when the second order closure of the 13 moment system is adopted, the solution not only presents a (single) subshock that is far less pronounced than that obtained with the linear closure – as predicted by the results illustrated in Fig. 1 – but the overall shock structure profile is arguably in far better agreement with the reference kinetic solution throughout the whole profile of the shock.

As anticipated in Section 4, an interesting peculiarity of the second order MEP closure of the 13 moment system, is that an analysis of the shock structure reveals that along the whole process the system does not exit the hyperbolicity region, at least for intensities of the shock parameter up to $M_0 \simeq 4$. This is in stark contrast to what happens with the traditional first order closure, where it is well documented [25] that $M_0 \simeq 2.7$ is a threshold value above which complex characteristic velocities are found (see also Fig. 2). The fact that in the case of the second order closure the characteristic velocities are always real, even for Mach number as large as $M_0 = 4$ is explained by noticing that the state of the system happens to be in all these cases in the hyperbolicity region denoted as I in the recent paper by Brini and Ruggeri [16].

7 Moment System of a Polyatomic Gas: $\mathbf{ET^1_{14}}$ and $\mathbf{ET^2_{14}}$

The RET of polyatomic gases is a relatively recent theory developed by Arima, Taniguchi, Ruggeri and Sugiyama at the macroscopic level [26]. This theory adopts two parallel hierarchies (binary hierarchy) for the following independent fields: mass density, velocity, internal energy, shear stress, dynamic pressure, heat flux. One hierarchy consists of balance equations for the mass density, the momentum density and the momentum flux (*momentum-like* hierarchy), and the other one consists of balance equations for the energy density and the energy flux (*energy-like* hierarchy):

$$
\begin{aligned}
&\partial_t F + \partial_i F_i = 0,\\
&\partial_t F_{k_1} + \partial_i F_{ik_1} = 0,\\
&\partial_t F_{k_1k_2} + \partial_i F_{ik_1k_2} = P_{k_1k_2},
\end{aligned}
\qquad\qquad
\begin{aligned}
&\partial_t G_{kk} + \partial_i G_{ikk} = 0,\\
&\partial_t G_{kkj} + \partial_i G_{kkij} = Q_{kkj},
\end{aligned}
$$

These hierarchies cannot merge with each other in contrast to the case of rarefied monatomic gases because the specific internal energy (the intrinsic part of the energy density) is no longer related to the pressure (one of the intrinsic parts of the momentum flux) in a simple way.

Concerning the kinetic counterpart, for rarefied polyatomic gases the main idea is to consider a distribution function $f(\mathbf{x}, \mathbf{c}, t, I)$ that depends on an extra variable I that takes into account the internal mode of the molecules (rotation and vibration). Its rate of change is determined by the Boltzmann equation which has the same form as the one of monatomic gases (1) but the collision integral $Q(f)$ takes into account the influence of the internal degrees of freedom through the collisional cross section.

Pavić, Ruggeri, and Simić [27] considered the case of 14 generalized moments

$$\begin{pmatrix} F \\ F_{k_1} \\ F_{k_1 k_2} \end{pmatrix} = \int_{\mathbb{R}^3} \int_0^\infty m \begin{pmatrix} 1 \\ c_{k_1} \\ c_{k_1} c_{k_2} \end{pmatrix} f(\mathbf{x}, \mathbf{c}, t, I)\, \varphi(I)\, dI\, d\boldsymbol{c},$$
$$\begin{pmatrix} G_{kk} \\ G_{kkj} \end{pmatrix} = \int_{\mathbb{R}^3} \int_0^\infty m \begin{pmatrix} c^2 + 2\frac{I}{m} \\ \left(c^2 + 2\frac{I}{m}\right) c_j \end{pmatrix} f(\mathbf{x}, \mathbf{c}, t, I)\, \varphi(I)\, dI\, d\boldsymbol{c}. \tag{37}$$

The weighting function $\varphi(I)$ is determined in such a way that it recovers the caloric equation of state in equilibrium for polyatomic gases.

More details can be read in the book by Ruggeri and Sugiyama that is completely devoted to the RET of polyatomic gases [5].

In the one-dimensional case, the 14 moment system of a polyatomic gas (37) may be written in the form of Eq. (16), with the following densities $\mathbf{u}$, fluxes $\mathbf{F}^1$ and production terms $\mathbf{P}$ [5]:

$$\mathbf{u} = \begin{pmatrix} F \\ F_1 \\ G_{kk} \\ F_{kk} \\ F_{\langle 11 \rangle} \\ G_{kk1} \end{pmatrix} = \begin{pmatrix} \rho \\ \rho v \\ \rho v^2 + 2\rho\varepsilon \\ \rho v^2 + 3\,(p + \Pi) \\ \frac{2}{3}\rho v^2 - \sigma \\ \rho v^3 + 2\,(p + \Pi - \sigma)\, v + 2\rho\varepsilon v + 2q \end{pmatrix},$$

$$\mathbf{F}^1 = \begin{pmatrix} \rho v \\ \rho v^2 + p + \Pi - \sigma \\ \rho v^3 + 2\rho\varepsilon v + 2\,(p + \Pi - \sigma)\, v + 2q \\ \rho v^3 + 5\,(p + \Pi - \sigma)\, v + 3\sigma v + \hat{F}_{kk1} \\ \frac{2}{3}\rho v^3 + \frac{4}{3}\,(p + \Pi - \sigma)\, v - \sigma v + \hat{F}_{\langle 11 \rangle 1} \\ \rho v^4 + 5\,(p + \Pi - \sigma)\, v^2 + 2\rho\varepsilon v^2 + 4qv + 2\hat{F}_{\langle 11 \rangle 1} v + \frac{2}{3}\hat{F}_{kk1} v + \hat{G}_{kk11} \end{pmatrix},$$

$$\mathbf{P} = \begin{pmatrix} 0 \\ 0 \\ 0 \\ \hat{P}_{kk} \\ \hat{P}_{\langle 11 \rangle} \\ 2\hat{P}_{11} v + \hat{P}_{kk1}, \end{pmatrix}.$$

In addition to the field variables already introduced in the context of the monatomic gas, the 14 moment system of a polyatomic gas contains the variable Π representing the dynamical pressure, which is identically null in the monatomic gas case.

In order to close the system, the intrinsic moments $\hat{F}_{kk1}$, $\hat{F}_{\langle 11 \rangle 1}$, $\hat{G}_{kk11}$ and the production terms $\hat{P}_{kk}$, $\hat{P}_{\langle 11 \rangle}$, $\hat{P}_{kk1}$ and $\hat{P}_{11} = \hat{P}_{\langle 11 \rangle} + \frac{1}{3} P_{kk}$ must be considered local functions of the field $\mathbf{u}$.

7.1 First Order Closure

The closure was obtained via MEP at first order in [27] for polytropic gas and recently in [28] in the case of non-polytropic gas.

For rarefied polytropic gas in which the pressure p and the internal energy ε in equilibrium are given by

$$p = \frac{k}{m}\rho T, \qquad \varepsilon = \frac{D}{2}\frac{k}{m}T,$$

the following expressions for the intrinsic moments was obtained [5, 27]:

$$\hat{F}^{(1)}_{kk1} = \frac{10}{D+2}\,q, \qquad \hat{F}^{(1)}_{\langle 11\rangle 1} = \frac{8}{3\,(D+2)}\,q,$$
$$\hat{G}^{(1)}_{kk11} = (D+2)\,\frac{p^2}{\rho} + (D+4)\,\frac{(\Pi-\sigma)\,p}{\rho},$$

where the constant D represents the total degrees of freedom of the polyatomic gas molecule.

7.2 Second Order Closure

Proceeding as in the case indicated in Section 3 for the case of monatomic gas it is possible to obtain the second order closure ($\alpha = 2$) provides the following expressions for the intrinsic moments $\hat{F}_{kk1}$, $\hat{F}_{\langle 11\rangle 1}$, $\hat{G}_{kk11}$, now denoted respectively as $\hat{F}^{(2)}_{kk1}$, $\hat{F}^{(2)}_{\langle 11\rangle 1}$, and $\hat{G}^{(2)}_{kk11}$:

$$\hat{F}^{(2)}_{kk1} = \frac{10}{D+2}\,q + \frac{20D}{(D+2)^2}\,\frac{\Pi q}{p} - \frac{8\,(D-3)}{(D+2)^2}\,\frac{\sigma q}{p},$$
$$\hat{F}^{(2)}_{\langle 11\rangle 1} = \frac{8}{3\,(D+2)}\,q + \frac{16D}{3\,(D+2)^2}\,\frac{\Pi q}{p} - \frac{4\,(7D+6)}{3\,(D+2)^2}\,\frac{\sigma q}{p},$$
$$\hat{G}^{(2)}_{kk11} = (D+2)\,\frac{p^2}{\rho} + (D+4)\,\frac{(\Pi-\sigma)\,p}{\rho} + \frac{4\,(5D+22)}{(D+2)^2}\,\frac{q^2}{p} + 2\frac{(\Pi-\sigma)^2}{\rho}.$$

In a paper in preparation [29] the second order closure was done also in the 3-dimensional case with the aim to evaluate the corresponding hyperbolicity domain. The non-zero components of the production term $\mathbf{P}$ that we shall adopt in the following are given by the following expressions [5]:

$$\hat{P}_{kk} = -\frac{3\Pi}{\tau_\Pi}, \qquad \hat{P}_{\langle 11\rangle} = \frac{\sigma}{\tau_\sigma}, \qquad \hat{P}_{kk1} = -\frac{2q}{\tau_q}.$$

When not explicitly stated otherwise, the relaxation times τ_Π, τ_σ, and τ_q (respectively related to the dynamic pressure, viscosity and heat conductivity) will be assumed to have the same value ($\tau = \tau_\Pi = \tau_\sigma = \tau_q$) as to allow a comparison of the results obtained numerically solving the 14 moment system with the results obtained from the solution of the Boltzmann/BGK kinetic model.

7.3 Numerical Results

A non-exhaustive numerical study of the shock structure solution with and without subshock for a polyatomic gas has been carried out in the case of a *pseudo*-N_2 gas, namely a N_2-like gas except for the three relaxation times being equal ($\tau = \tau_{\Pi} = \tau_{\sigma} = \tau_q$). This over-simplifying assumption, which is not physically realistic[1], is merely made as to allow a comparison of the results obtained in the framework of the 14 moment system with the results obtained solving the kinetic equation of the Boltzmann/BGK model. The kinetic model of a polyatomic gas employed here is based on the polyatomic gas model recently presented and discussed in [27] (see also [5] and references therein). The details concerning the numerical algorithm developed for the solution of the Boltzmann/BGK equation for polyatomic gas shall be the subject of a forthcoming paper and will not be discussed here.

In Fig. 6, the case of a shock structure characterized by the unperturbed Mach number $M_0 = 1.47$ is presented. Since this value of M_0 is less than the critical value $M_0^{cr} \simeq 1.74$ corresponding to a shock speed s equal to the maximum characteristic velocity of the system in the unperturbed state [30], no subshock is expected to appear in the solution. The density and velocity fields computed numerically, shown in Fig. 6, clearly represent a continuous shock structure profile, thus confirming the theoretical prediction.

The shock structure profile obtained with $M_0 = 2$, shown in Fig. 7, is characterized by a noticeable discontinuity in the shock structure profile. It is noted that the numerical results resemble the results obtained for a monatomic gas both qualitatively and quantitatively: As seen in the case of a monatomic gas, the strength of the subshock jump found when the second order closure is adopted, is smaller than the one obtained with the traditional linear closure, and overall the numerical solution obtained with the second order closure is arguably closer to the reference solution obtained by means of the kinetic approach, than the numerical solution obtained with the linear closure.

The same behavior is found when the Mach number is further increased to $M_0 = 3$, as shown in Fig. 8. Similarly to the monatomic gas case, a second order closure leads to a shock structure profile characterized by a remarkably smaller subshock jump, and with an overall behavior that matches better the reference result obtained when the kinetic model equation is solved.

In recent years much research work has been devoted to the analysis of the shock structure in polyatomic gases [5, 31–35]. It is now understood that for several polyatomic gases relevant in practical applications, as for example carbon dioxide (CO_2), the dynamic pressure plays a relevant role in non-equilibrium processes, and the model assumption of a single relaxation time for all the involved relaxation processes is not acceptable when the fine structure of processes far from equilibrium is of interest.

[1] For N_2 gas, the relaxation time τ_{Π} is several orders of magnitude larger than τ_{σ} and τ_q.

In particular, it was predicted by non-equilibrium models and observed in experiments, that for polyatomic gases like CO_2, the shock structure profile has a peculiar behavior which substantially differs from the one observed in monatomic gases: the shock structure is characterized in fact, for values of the shock speed smaller than the maximum characteristic speed of the system in the unperturbed equilibrium state, by a very sharp (but continuous) part of the profile, followed by a much less sharp part of the profile. This peculiar feature of the shock profile was obtained both in the framework of extended thermodynamics [31] and in the context of kinetic theory [33, 34]. The results presented in [31, 33] are replicated in Fig. 9, and are accompanied by simulation results obtained in the context of the present study by means of the 14 moment system model with the first and second order closures. These preliminary numerical results seem to suggest that, in this case, a second order closure is not beneficial in terms of an improvement in the shock structure profile. This result is not surprising and has to be expected, since it was clearly shown [32–34] that the traditional linear closure already provides predictions that are in excellent agreement with the results obtained with kinetic models, and experimentally found, leaving as a matter of fact very small room for improvements.

In this particular case study, even the investigation of the fine structure of the steep part of the profile of the shock structure, show virtually no difference in the results obtained in the framework of the 14 moment system with either first or second order closure, at least in the case reported in Fig. 9 concerning a shock with an unperturbed Mach number $M_0 = 1.47$ below the critical value above which a subshock is expected.

8 Conclusions

The closure of the 13 moment system of a monatomic gas is generally obtained assuming a linear dependence of the closing fluxes on the non-equilibrium variables, i.e. the shear stress and heat flux. In the framework of Rational Extended Thermodynamics (RET), this closure is obtained by means of the entropy principle, with a phenomenological approach, or equivalently by means of the maximum entropy principle (MEP). Either way, the obtained closure is equivalent to the closure obtained by Grad following a kinetic approach. The resulting 13 moment system has been largely used in theoretical investigation of non-equilibrium phenomena as well as in studies concerning practical applications, but it suffers from some well-known drawbacks, most notably the lack of hyperbolicity and the occurrence of non-physical shocks when processes far from equilibrium are involved.

For example, when the shock structure solution is analyzed, for a large enough departure from equilibrium (i.e. for large Mach numbers), an unphysical subshock appears in the profile of the traveling wave. This latter well-known feature of the 13 moment system is a prominent issue when it comes to study

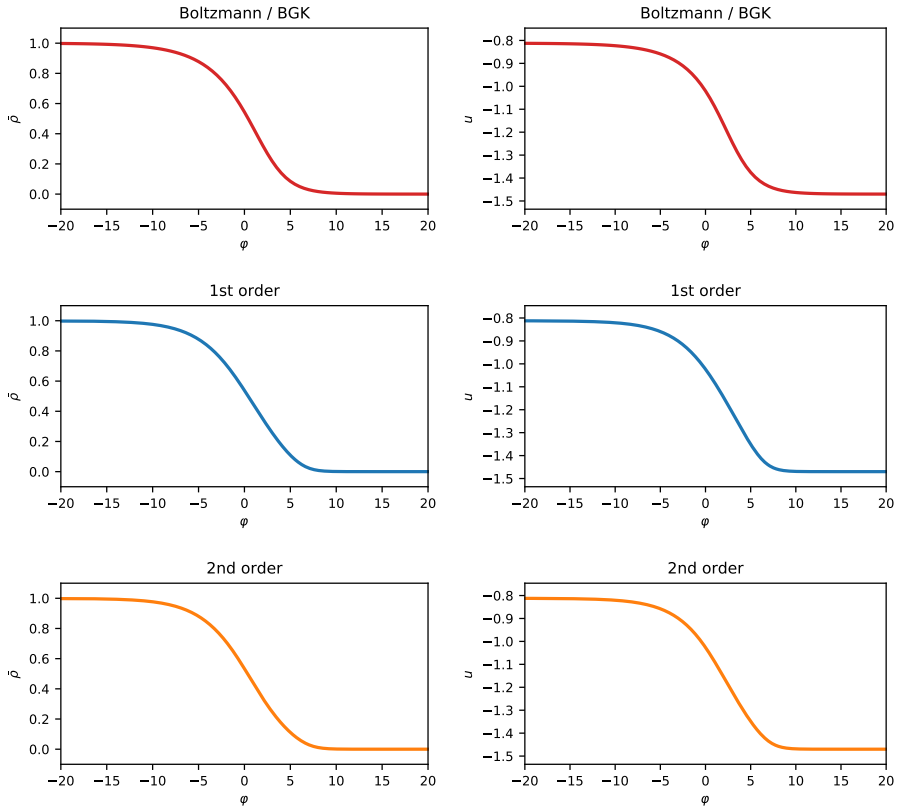

Fig. 6 Rescaled mass density profile $\bar{\rho} = (\rho - \rho_0)/(\rho_1 - \rho_0)$ (on the left) and relative velocity profile $u = v - s$ (on the right) of the shock structure solution obtained for $M_0 = 1.5$ in a polyatomic gas ($D = 5$; *pseudo*-N_2 gas with $\tau = \tau_\Pi = \tau_\sigma = \tau_q$) with the Boltzmann/BGK model (top row), and with the 14 moment system with the first order MEP closure (middle row) and second order MEP closure (bottom row).

the propagation of shock waves in real gases and the fine structure of the shock profile is of interest.

An investigation on the features of the shock structure solution of the 13 moment system with a second order closure based on the maximum entropy principle (MEP) closure is here presented, and the results are compared and contrasted to those obtained with the traditional first order closure. Most notably, it is seen that the subshock that appears in the shock structure profile for large enough Mach numbers is greatly reduced when the second order closure is exploited. This remarkable result is obtained on the basis of the Rankine-Hugoniot compatibility conditions applied across the subshock, and it is confirmed by explicit numerical solution of the system of ordinary differential equations that result from the system of moment equations when a shock structure solution is sought. The comparison of the numerical results to those

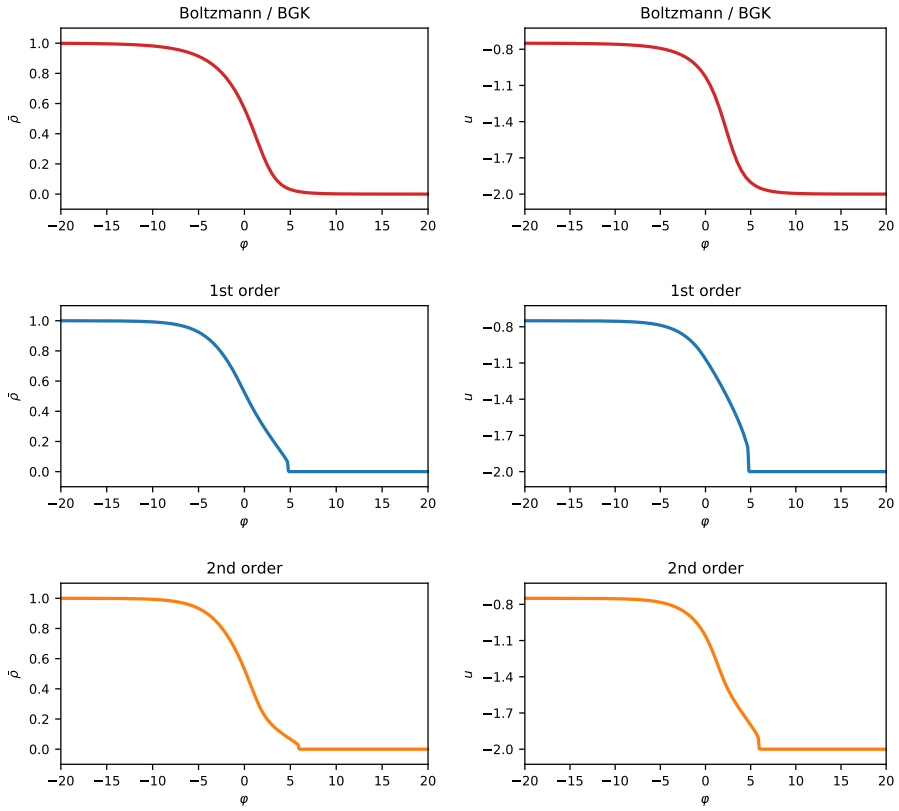

Fig. 7 Rescaled mass density profile $\bar{\rho} = (\rho - \rho_0) / (\rho_1 - \rho_0)$ (on the left) and relative velocity profile $u = v - s$ (on the right) of the shock structure solution obtained for $M_0 = 2.0$ in a polyatomic gas ($D = 5$; *pseudo*-N_2 gas with $\tau = \tau_\Pi = \tau_\sigma = \tau_q$) with the Boltzmann/BGK model (top row), and with the 14 moment system with the first order MEP closure (middle row) and second order MEP closure (bottom row).

obtained solving the kinetic Boltzmann/BGK equation, considered here as a reference solution, show that a second order MEP-based closure allows to obtain shock structure profiles that are in general more satisfactory than those obtained with the traditional first order closure.

In addition, a preliminary analysis of the case of the 14 moment system of a polyatomic gas is introduced. The study presented here pertains to a pseudo-N_2 polyatomic gas, and suggests that also for this kind of polyatomic gas the obtained results are qualitatively similar to those obtained for a monatomic gas. The more interesting and physically relevant case of a polyatomic gas with different relaxation times (in particular, the relaxation time for the dynamic pressure can be three to four order of magnitude larger than the other relaxation times, for gases like CO_2) is addressed as well. In this case, recent theoretical and computational results have pointed out that the continuous

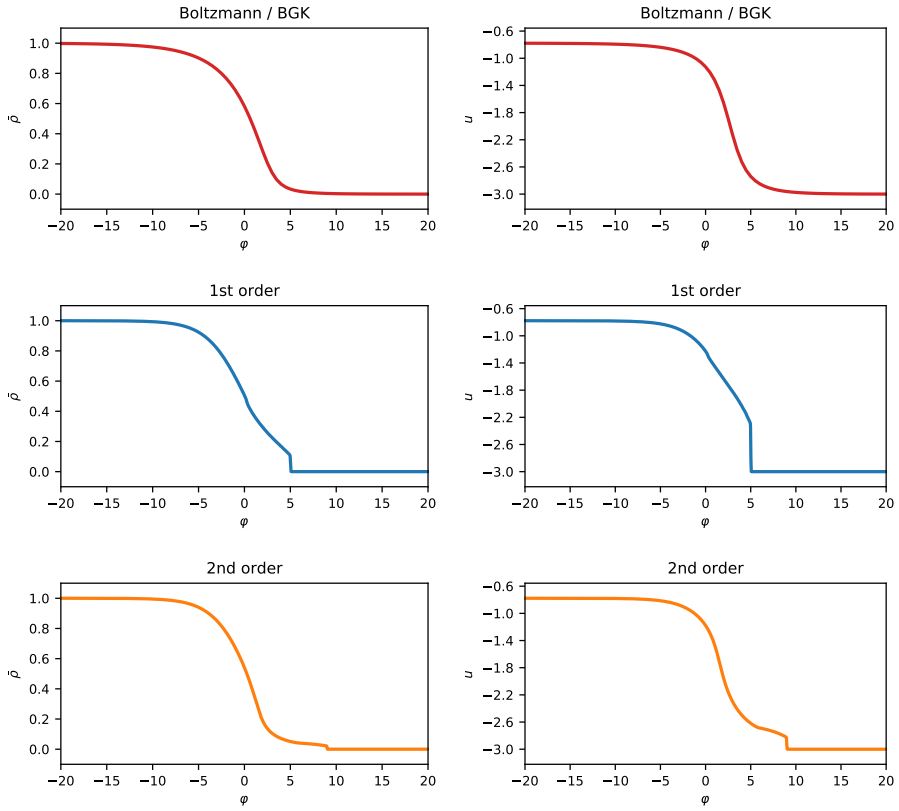

Fig. 8 Rescaled mass density profile $\bar{\rho} = (\rho - \rho_0)/(\rho_1 - \rho_0)$ (on the left) and relative velocity profile $u = v - s$ (on the right) of the shock structure solution obtained for $M_0 = 3.0$ in a polyatomic gas ($D = 5$; *pseudo*-N_2 gas with $\tau = \tau_\Pi = \tau_\sigma = \tau_q$) with the Boltzmann/BGK model (top row), and with the 14 moment system with the first order MEP closure (middle row) and second order MEP closure (bottom row).

shock structure solution, has a peculiar behavior substantially different from the one found in monatomic gases. In particular, for these polyatomic gases it was found that the system of moment equations provided by the theory of extended thermodynamics with linear closure are in a remarkably good agreement with the experimental results, even for small number of moments (in particular, it was observed that the ET6 theory, which is the simplest non-equilibrium theory involving only six field (i.e. the mass density ρ, the velocity $\mathbf{v}$, the temperature T and the dynamic (non-equilibrium) pressure Π), already provides results in outstanding agreement with the experiments). In this cases, it has to be expected that a second order closure would not lead to noticeable benefit as long as prediction of the shock structure solution is concerned. The results reported here confirm this expectation, showing that the shock structure profile computed with a first and second order closures are virtually

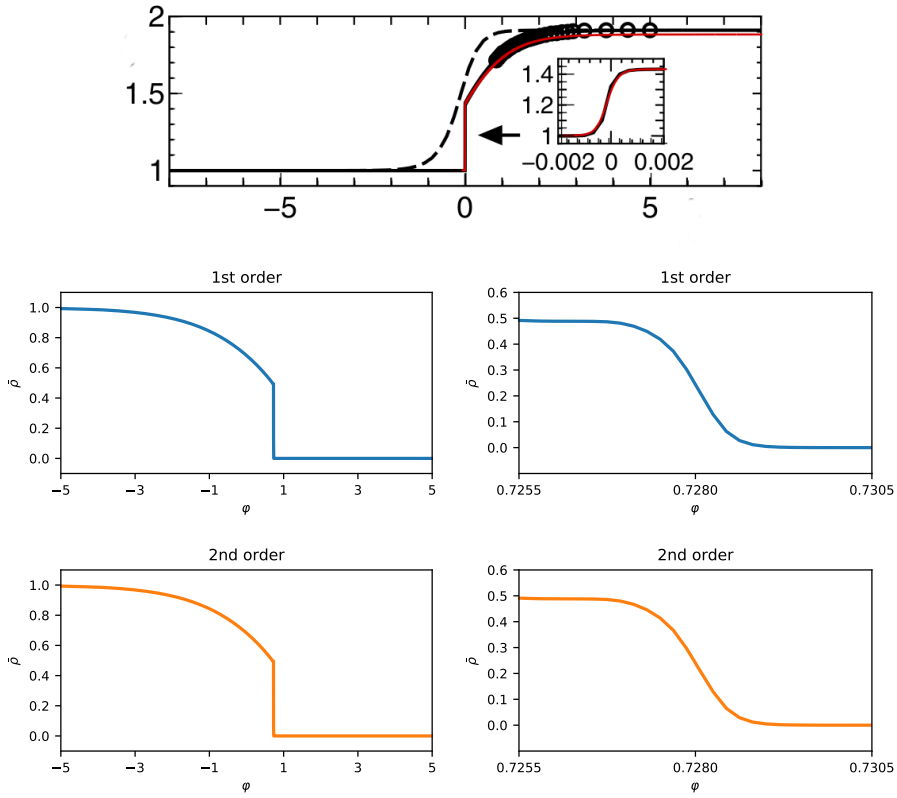

Fig. 9 Reproduction of the results published in [33] obtained for a shock profile in a CO_2 polyatomic gas with $M_0 = 1.47$ (top row) and corresponding rescaled mass density profile $\bar{\rho} = (\rho - \rho_0)/(\rho_1 - \rho_0)$ (middle and bottom row; on the left) with its magnification (on the right) of the shock structure solution obtained with the 14 moment system with the first order MEP closure (middle row) and second order MEP closure (bottom row).

indistinguishable, at least for shock structures characterized by small values of the strength of the shock.

One final comment is in order. The analysis discussed in this paper is focused on the one-dimensional shock structure problem, which serves as a good benchmark for non-equilibrium theories.

Nevertheless, to be useful for relevant practical applications, an extension to more useful two- and three-dimensional models, possibly with finite domains, is desirable. Despite such an extension is certainly feasible and, in principle, can be done with a straightforward generalization of the procedure described here, such an extension is beyond the scope of the present study. It should be noted, however, that even if the one-dimensional shock structure problem studied here can already be analyzed by means of the powerful approach of kinetic theory (which indeed served as a reference model throughout the paper), the macroscopic approach of the moment equations with second

and potentially even higher order closures [17], still have an edge over the kinetic theory approach, being far less computationally demanding. The reduced computational cost is sensible for the one-dimensional case exposed here and it is expected to be even more dramatic for two- and three-dimensional situations, especially when the time-evolution of the solution is of interest.

Acknowledgments

This work was partially supported by GNFM/INdAM; one of the authors (A.M.) was also partially supported by the Italian MIUR *PRIN2017* project "Multiscale phenomena in Continuum Mechanics: singular limits, off-equilibrium and transitions"(project number: 2017YBKNCE).

References

1. Cercignani C.: The Boltzmann Equation and Its Applications, Springer-Verlag, New York (1988)
2. Sone Y.: Kinetic Theory and Fluid Dynamics, Birkhäuser, Boston (2002)
3. Sone Y.: Molecular Gas Dynamics, Theory, Techniques, and Applications, Birkhäuser, Boston (2007)
4. Müller, I., Ruggeri, T.: Rational Extended Thermodynamics. Springer, New York (1998)
5. Ruggeri, T., Sugiyama, M.: Rational Extended Thermodynamics Beyond the Monatomic Gas. Springer, Basel (2015)
6. Grad, H.: On the kinetic theory of rarefied gases. Commun. Pure Appl. Math. **2**, 331–407 (1949)
7. Dreyer, W.: Maximization of the entropy in non-equilibrium. J. Phys. A Math. Gen. **20**, 6505–6517 (1987)
8. Müller, I. Ruggeri, Extended Thermodynamics. Springer, New York (1993)
9. Jaynes, E. T.: Information theory and statistical mechanics. Phys. Rev. **106**, 620–630 (1957)
10. Jaynes, E. T.: Information theory and statistical mechanics II. Phys. Rev. **108**, 171–190 (1957)
11. Kogan, M. N.: Rarefied Gas Dynamics. Plenum Press, New York (1969)
12. Boillat, G., Ruggeri, T.: Moment equations in the kinetic theory of gases and wave velocities. Contin. Mech. Thermodyn. **9**, 205–212 (1997)
13. Levermore, C. D.: Moment closure hierarchies for kinetic theories. J. Stat. Phys. **83**, 1021–1065 (1996)
14. Junk, M.: Domain of Definition of Levermore's Five-Moment System. J. Stat. Phys. **93**, 1143–1167 (1998)
15. Boillat, G., Ruggeri, T.: On the Shock Structure Problem for Hyperbolic System of Balance Laws and Convex Entropy. Contin. Mech. Thermodyn. **5**, 285–292 (1998)
16. Brini, F., Ruggeri, T.: Second-order approximation of extended thermodynamics of a monatomic gas and hyperbolicity region. Contin. Mech. Thermodyn. **32**, 23–39 (2020)
17. Mentrelli, A.: Shock structure in the 14 moment system of extended thermodynamics with high order closure based on the maximum entropy principle. Ric. Mat., DOI: 10.1007/s11587-020-00511-x (2020)
18. Brini, F., Ruggeri, T.: Entropy principle for the moment systems of degree α associated to the Boltzmann equation. Critical derivatives and non controllable boundary data. Contin. Mech. Thermodyn. **14**, 165–189 (2002)
19. Ruggeri, T., Strumia, A.: Main field and convex covariant density for quasi-linear hyperbolic systems. Relativistic fluid dynamics. Ann. Inst. H. Poincaré Sect. A **34**, 65–84 (1981)

20. Ruggeri, T.: Galilean invariance and entropy principle for systems of balance laws. Contin. Mech. Thermodyn. **1**, 3–20 (1989)
21. Ruggeri T.: Godunov Symmetric Systems and Rational Extended Thermodynamics. In Contin. Mechanics, Applied Mathematics and Scientific Computing: Godunov's Legacy. Demidenko, G.V., Romenski, E., Toro, E., Dumbser, M. (Eds.). ISBN 978-3-030-38869-0 (2020)
22. Boillat, G., Ruggeri T.: Hyperbolic Principal Subsystems: Entropy Convexity and Subcharacteristic Conditions, Arch. Rational Mech. Anal., **137**, 305-320 (1997)
23. Junk, M.: Maximum entropy for reduced moment problems. Math. Models Methods Appl. Sci. **10**, 1001–1025 (2000)
24. Weiss W.: Continuous shock structure in extended thermodynamics. Phys. Rev. E **52**, R5760–R5763 (1995)
25. Ruggeri, T.: Shock Waves in Hyperbolic Dissipative Systems in "Nonlinear waves and dissipative effects" (Proceedings of the Euromech Colloquium 270; Reggio Calabria, 25-28 September 1990), Eds. D. Fusco, A. Jeffrey Pitman Research Notes in Mathematical Series, Vol. 227; Longman Scientific & Technical, 256-264 (1991)
26. Arima, T., Taniguchi, S., Ruggeri, T., Sugiyama, M.: Extended thermodynamics of dense gases. Continuum Mech. Thermodyn. **24**, 271-292 (2011)
27. Pavić M., Ruggeri T., Simić S.: Maximum entropy principle for rarefied polyatomic gases. Physica A **392**, 1302–1317 (2013)
28. Ruggeri, T.: Maximum entropy principle closure for 14-moment system for a non-polytropic gas, Ric. Mat., DOI: 10.1007/s11587-020-00510-y (2020)
29. Brini F., Ruggeri T.: Second-order approximated extended thermodynamics theory of polytropic rarefied gases and its hyperbolicity property. In preparation.
30. Arima T., Taniguchi S., Ruggeri T., Sugiyama M.: Monatomic rarefied gas as a singular limit of polyatomic gas in extended thermodynamics. Phys. Lett. A **377**, 2136–2140 (2013)
31. Taniguchi S., Arima T., Ruggeri T., Sugiyama M.: Thermodynamic theory of the shock wave structure in a rarefied polyatomic gas: Beyond the Bethe-Teller theory. Phys. Rev. E **89**, 013025 (2014)
32. Taniguchi S., Arima T., Ruggeri T., Sugiyama M.: Shock wave structure in rarefied polyatomic gases with large relaxation time for the dynamic pressure. J. Phys.: Conf. Ser. **1035**, 012009 (2018)
33. Kosuge S., Aoki K.: Shock-wave structure for a polyatomic gas with large bulk viscosity. Phys. Rev. Fluids **3**, 023401-1/42 (2018)
34. Kosuge S., Kuo, H.-W., Aoki K.: A kinetic model for a polyatomic gas with temperature-dependent specific heats and its application to shock-wave structure. J. Stat. Phys. **177**, 209–251 (2019)
35. Ruggeri T., Taniguchi S.: Shock Waves in Hyperbolic Systems of Non-Equilibrium Thermodynamics. Applied Wave Mathematics II: Selected Topics in Solids, Fluids, and Mathematical Methods and Complexity (Volume dedicated to Juri Engelbrecht on his 80th birthday). Mathematics of Planet Earth 6 (Eds. A. Berezovski, T. Soomere), Springer Verlag, pp. 167–186, DOI: 10.1007/978-3-030-29951-4_8 (2019)